Interaction of the HOPS complex with Syntaxin 17 mediates autophagosome clearance in *Drosophila*

Szabolcs Takáts[a],*, Karolina Pircs[a],*, Péter Nagy[a], Ágnes Varga[a], Manuéla Kárpáti[a], Krisztina Hegedűs[a], Helmut Kramer[b], Attila L. Kovács[a], Miklós Sass[a], and Gábor Juhász[a]
[a]Department of Anatomy, Cell and Developmental Biology, Eötvös Loránd University, Pazmany s. 1/C, H-1117 Budapest, Hungary; [b]Department of Neuroscience, Department of Cell Biology, University of Texas Southwestern Medical School, Dallas, TX 75390-9111

ABSTRACT Homotypic fusion and vacuole protein sorting (HOPS) is a tethering complex required for trafficking to the vacuole/lysosome in yeast. Specific interaction of HOPS with certain SNARE (soluble NSF attachment protein receptor) proteins ensures the fusion of appropriate vesicles. HOPS function is less well characterized in metazoans. We show that all six HOPS subunits (Vps11 [vacuolar protein sorting 11]/CG32350, Vps18/Dor, Vps16A, Vps33A/Car, Vps39/CG7146, and Vps41/Lt) are required for fusion of autophagosomes with lysosomes in *Drosophila*. Loss of these genes results in large-scale accumulation of autophagosomes and blocks autophagic degradation under basal, starvation-induced, and developmental conditions. We find that HOPS colocalizes and interacts with Syntaxin 17 (Syx17), the recently identified autophagosomal SNARE required for fusion in *Drosophila* and mammals, suggesting their association is critical during tethering and fusion of autophagosomes with lysosomes. HOPS, but not Syx17, is also required for endocytic down-regulation of Notch and Boss in developing eyes and for proper trafficking to lysosomes and eye pigment granules. We also show that the formation of autophagosomes and their fusion with lysosomes is largely unaffected in null mutants of Vps38/UVRAG (UV radiation resistance associated), a suggested binding partner of HOPS in mammals, while endocytic breakdown and lysosome biogenesis is perturbed. Our results establish the role of HOPS and its likely mechanism of action during autophagy in metazoans.

INTRODUCTION

Eukaryotic cells have developed distinct membrane-bound compartments with specific functions. Trafficking from one compartment to the other is usually achieved by the fusion of transport vesicles with their target. This process is mediated by complex molecular machineries that ensure proper movement, tethering, and specific fusion of various vesicles. A combination of signals establishes vesicle identity, including the lipid content of the limiting membrane (such as the presence of various phospholipids) and members of the Rab family of small GTPases (Stenmark, 2009). Tethering factors are involved in vesicle docking, and fusion of the vesicle with the appropriate target membrane is usually mediated by SNARE (soluble NSF attachment protein receptor) protein complexes, formed by four (Qa, Qb, Qc, and R) SNARE domains (Hong, 2005).

Much of our understanding of these processes comes from yeast studies. Genetic screens carried out in the 1980s identified the first set of genes required for transport from the Golgi to the vacuole, the yeast equivalent of the lysosomal system (Bankaitis *et al.*, 1986; Rothman and Stevens, 1986; Bowers and Stevens, 2005). All these vacuolar protein sorting (*VPS*) mutants secrete

carboxypeptidase Y (CPY), which is a soluble vacuolar hydrolase in wild-type cells. *VPS* genes were classified based on the morphology of vacuoles in mutant cells (Bowers and Stevens, 2005). The class C group is characterized by the lack of a coherent vacuole and includes the genes *VPS11*, *VPS16*, *VPS18*, and *VPS33*. Mutants that belong to the class B group show numerous, small, fragmented vacuoles, and include *VPS39* and *VPS41*, among other genes. Biochemical studies established that these six gene products form a protein complex, which was named HOPS for <u>ho</u>motypic fusion and vacuole <u>p</u>rotein <u>s</u>orting. A separate complex termed CORVET (for class C <u>c</u>ore <u>v</u>acuole/<u>e</u>ndosome <u>t</u>ethering) was also described, which contains Vps3 and Vps8 instead of Vp39 and Vps41 (Balderhaar and Ungermann, 2013; Solinger and Spang, 2013). These complexes act as tethering factors by cross-linking two membranes, and also facilitate the formation of a SNARE complex during fusion. HOPS is not only required for the delivery of vacuolar proteins and homotypic fusion of vacuoles, but also appears to control the clearance of late endosomes and autophagosomes during heterophagy and autophagy through promoting fusion of these vesicles with the vacuole in yeast (Rieder and Emr, 1997). These pathways mediate the uptake and degradation of endocytosed extracellular material and receptor-ligand complexes, and the delivery of dispensable cytoplasmic material for breakdown, respectively. In contrast, CORVET was suggested to be involved in the maturation of early endosomes to late endosomes (Balderhaar and Ungermann, 2013; Solinger and Spang, 2013).

The function of these complexes is less well characterized in metazoan cells (Balderhaar and Ungermann, 2013; Solinger and Spang, 2013). Although clear homologues of *VPS8* are found, *VPS3* is not conserved. Studies in animals are also complicated by gene redundancy, as two homologues of *VPS16* and *VPS33* are found in worms, flies, and mammals. A complex containing VPS16A and VPS33A has been proposed to function similarly to HOPS in yeast, while a complex containing VPS16B and VPS33B has been speculated to play a role similar to that of CORVET (Balderhaar and Ungermann, 2013). These complexes play important roles in numerous biological processes in mammals, including antigen presentation and elimination of microbes in immune cells, and protection from various diseases causing neurodegeneration and multiorgan pathologies (Balderhaar and Ungermann, 2013; Solinger and Spang, 2013).

Several classical eye color mutant phenotypes in *Drosophila* turned out to be the result of mutations in genes encoding HOPS subunits (Lloyd *et al.*, 1998). These genes were named according to the phenotypes of mutant adult flies: *Vps18* is known as *dor* (*deep orange*), *Vps33A* as *car* (*carnation*), and *Vps41* as *lt* (*light*) in flies. These hypomorphic mutations perturb the biogenesis of eye pigment granules at the end of metamorphosis, whereas stronger mutations in these genes lead to lethality during earlier developmental stages. Loss of *dor* or *car* or hypomorphic mutation of *lt* also leads to defects in endocytosis, and similar phenotypes have been reported based on RNA interference (RNAi) analysis of *Vps16A* (Sevrioukov *et al.*, 1999; Pulipparacharuvil *et al.*, 2005; Akbar *et al.*, 2009; Swetha *et al.*, 2011). In contrast, *Vps16B/fob* (*full of bacteria*) appears to regulate the maturation of phagosomes containing endocytosed bacteria, and it is dispensable for receptor down-regulation (Akbar *et al.*, 2011). These studies suggest that distinct HOPS complexes may be responsible for different functions in animals.

During autophagy, fusion of double-membrane autophagosomes with lysosomes is required to deliver the sequestered cytoplasmic cargo for degradation. Autophagy has been implicated in a wide variety of physiological and pathological conditions (Mizushima

et al., 2008). In yeast, the SNARE proteins Vam3, Vti1, and Vam7 are involved in the direct fusion of autophagosomes with the vacuole (Darsow *et al.*, 1997; Wang *et al.*, 2002). Interestingly, metazoan cells seem to rely on a different trafficking route that appears to be critical: the fusion of autophagosomes with late endosomes to form intermediate vesicles called amphisomes, which then fuse with lysosomes (Filimonenko *et al.*, 2007; Rusten *et al.*, 2007; Juhasz *et al.*, 2008). In addition, among the SNAREs required for autophagosome clearance in yeast, only Vti1 has a clear homologue in animal cells, but not Vam3 or Vam7. We and others have recently identified Syntaxin 17 (Syx17 in *Drosophila* and STX17 in mammals) as the autophagosomal SNARE in metazoans, which forms a complex with ubisnap (Qbc, SNAP29 in mammals) and Vamp7 (R, VAMP8 in mammals) located on late endosomes and lysosomes (Itakura *et al.*, 2012; Takats *et al.*, 2013).

Whether and how HOPS is involved in autophagy in metazoans is not entirely clear, given that the SNAREs required for autophagosome-lysosome fusion are different from those in yeast. The possible involvement of HOPS in mammalian autophagy is controversial. Neuron-specific deletion of Vps18 was recently shown to cause neurodegeneration due to impaired biosynthetic, endocytic, and autophagic transport to lysosomes (Peng *et al.*, 2012). In contrast, Vps16 depletion by short hairpin RNA in mouse embryonic fibroblasts was found to delay the degradation of epidermal growth factor receptor (EGFR), a widely used endosomal cargo, but did not affect green fluorescent protein (GFP)-LC3 lipidation or puncta formation (Ganley *et al.*, 2011). In *Drosophila*, it was shown that *Vps16A* RNAi induced in the developing eye results in retinal degeneration, and ultrastructural images of dying photoreceptor cells in these animals revealed various vacuoles, including double-membrane autophagosomes, but the identity of these organelles was not further characterized (Pulipparacharuvil *et al.*, 2005). Another report showed that in viable *dor[1]* hypomorphic mutants, the size of LysoTracker Red (LTR)- and lysosome-associated membrane protein (Lamp1)-positive autolysosomes is decreased and the number of autophagosomes is increased during developmental autophagy of the fat body (Lindmo *et al.*, 2006). Interestingly, insulin signaling was up-regulated in those larvae, and levels of the molting hormone ecdysone, which is responsible for inducing developmental autophagy (Rusten *et al.*, 2004), remained low in wandering animals. These results suggest that systemic hormonal defects may contribute to autophagy phenotypes in these mutant animals (Lindmo *et al.*, 2006). The autophagic cargo p62/Ref2P was also found to be up-regulated in *dor[1]* but not in *car[1]* mutant adult heads (Bartlett *et al.*, 2011). Importantly, mutations used in these studies are hypomorphic alleles: *dor[1]* carries a C979Y amino acid change, while *car[1]* has L26V and G249V changes. Thus these point mutations may interfere with some but not all functions of these genes. This is further indicated by the lethality of *car* and *dor* null mutants during the first and second larval stages (Sevrioukov *et al.*, 1999; Akbar *et al.*, 2009).

In this work, we analyze the role of HOPS in autophagosome-lysosome fusion in *Drosophila*. Our results help in resolving the conflicting and inconsistent reports on the potential involvement of this complex in autophagy in the cells of a metazoan organism.

RESULTS

Novel mutations of *Vps16A* reveal its role in autophagosome clearance

We screened a collection of P element–bearing larval-lethal *Drosophila* strains for mutants with defects in developmental autophagy, and recently published the characterization of two hits

from our screen (Lippai *et al.*, 2008; Csikos *et al.*, 2009). In these papers, we showed that loss of AMPK (AMP-activated kinase) or epsin interferes with the formation of autophagosomes. Homozygous mutants of another candidate line, *l(3)S007902* (later named *Vps16A[FUD]*, see below), showed a complete block of punctate LTR staining in fat body cells of wandering L3-stage animals (Figure 1, A, B, and K). It is important to emphasize that the LTR dots appear only in response to starvation or in wandering larvae, and no such LTR-positive structures are detected in fat bodies of well-fed *Drosophila* larvae; therefore LTR staining is commonly used as a marker for autolysosomes in this tissue (Scott *et al.*, 2004; Takats *et al.*, 2013). Transmission electron microscopy revealed that the cytoplasm of these cells is filled with typical double-membrane autophagosomes (Figure 1, C and D). This very characteristic phenotype raised the possibility of a specific impairment of autophagosome fusion with late endosomes and lysosomes in mutant larvae.

Transposase-mediated excision of the inserted P element in *l(3)S007902* failed to restore wild-type autophagy, and these revertant lines still died as late L3 larvae, similar to the original mutants. Furthermore, the mutation causing autophagy defects and larval lethality could be separated from the P element insertion by recombination. These genetic tests indicated that impaired autophagy and larval lethality are due to the presence of a background mutation on the P element–bearing chromosome. We thus named this unknown mutation *FUD* (*FUsion Defective*). Recombination and deletion mapping placed this mutation to the 85D7 region on the third chromosome, based on its failure to complement the deficiency lines *Df(3R)ED5339* and *Df(3R)BSC507*. One of the genes located in the overlapping region of these deficiencies, *Vps16A*, encoding a subunit of HOPS complex, seemed to be the most likely candidate potentially involved in autophagosome fusion events. Sequencing the locus identified a mutation at the 3′ end of the third intron in *FUD* mutants, changing the last three nucleotides from CAG to GAG (Figure 1E), which likely interferes with the proper splicing of *Vps16A*. To confirm the role of *Vps16A* in autophagy, we generated targeted deletions by improper excision of the P element *GS5053*, inserted in the 5′ untranslated region of the gene, 64 nucleotides upstream of the translational start site ATG. The new alleles remove 926 (*d116*) and 1105 (*d32*) nucleotides starting from the P element insertion site, deleting the protein-coding sequences in exons 1–3 and parts of exon 4 (Figure 1E). Animals transheterozygous for these alleles and a large chromosomal deficiency also die as late L3 stage larvae.

All three *Vps16A* alleles prevented LTR puncta formation in fat bodies of starved mutants (Figure 1, F–H, J, and L). As transgenic expression of wild-type *Vps16A* completely restored viability and starvation-induced LTR dot formation in *Vps16A^d32* mutant animals (Figure 1, I and L), we concluded that the loss of *Vps16A* is responsible for these mutant phenotypes. In line with that, no Vps16A protein could be detected in *Vps16A^d32* or *Vps16A^d116* mutants, while a faint band was visible in *Vps16A^FUD* (Figure 1M), suggesting these deletions represent null alleles and *Vps16A^FUD* is a strong hypomorphic mutation. Levels of the selective autophagy cargo p62 (also known as Ref2P in flies) are widely used for monitoring autophagy (Pircs *et al.*, 2012). Accumulation of p62 was obvious in Western blots of all three *Vps16A* mutants, similar to highly increased levels of autophagosome-associated, lipidated Atg8a-II (autophagy-related 8a; Figure 1M), in line with impaired autophagosome clearance. As expected, transgenic expression of wild-type *Vps16A* restored normal levels of Vps16A, p62, and Atg8a-II in all three mutant lines (Figure 1M).

All six subunits of the HOPS complex are required for autophagosome clearance

These data prompted us to systematically analyze the role of individual HOPS subunits in autophagy. We generated RNAi-expressing somatic cell clones (marked by coexpression of GFP) in starved larvae expressing mCherry-Atg8a in the fat body. This reporter labels autophagosomes as well as autolysosomes due to persisting fluorescence of the mCherry tag inside acidic lysosomes. Knockdown of *Vps16A*, *car*, *dor*, *Vps39/CG7146*, *Vps11/CG32350*, or *lt* produced a very similar phenotype: faint, small, mCherry-positive dots accumulated in the perinuclear region of cells, unlike the brighter and bigger puncta observed in the cytoplasm of neighboring control cells (Figure 2, A and B, and Supplemental Figure S1, A–E). The variability seen in the number and size of mCherry-Atg8a structures in control cells among different genotypes is likely due to biological variability, which affects different animals or cohorts of animals. Some of these discrepancies may also be caused by slight differences in setting the appropriate signal intensity threshold when extracting dot size and number data during image analysis. Note that, in these and all subsequent mosaic experiments, genetically manipulated cells are compared with their neighboring cells in the same tissue of the same animal, which serve as a built-in control, so the control and RNAi (or mutant) data pairs are essentially linked together.

In cell clones marked by Lamp1-GFP, which also express RNAi transgenes to silence the genes encoding HOPS subunits, starvation failed to induce discernible dots of LTR (Figures 2, C and F, and S1, F–J). Similar to *Vps16A* mutants, punctate LTR staining was inhibited in a *Vps11* mutant line that harbors a transposon insertion in the 5′ untranslated region of this gene and in *lt* mutant larvae (Figure 2, D, E, and G). To further characterize these loss-of-function phenotypes, we used a tandem mCherry- and GFP-tagged Atg8a reporter of autophagic flux (Kimura *et al.*, 2007; Takats *et al.*, 2013). In control cells of starved larvae, these reporter molecules are transported by autophagy to lysosomes in which GFP is rapidly quenched but mCherry fluorescence persists (Figure 2H). Knockdown of *Vps16A*, *car*, *dor*, *Vps39/CG7146*, *Vps11/CG32350*, or *lt* strongly interfered with autophagic flux: although a large number of mCherry-GFP-positive dots were formed, these remained double positive (Figures 2I and S2), suggesting autophagosomes are unable to mature into autolysosomes in these cells. Immunofluorescence labeling of endogenous Atg8a revealed large-scale accumulation of autophagosomes in *Vps16A*, *dor*, or *car* mutant fat body cell clones of starved larvae (Figure 3, A, C, E, and G). Furthermore, both the number and size of endogenous p62 aggregates increased in these cells (Figure 3, B, D, F, and H). A similar accumulation of punctate Atg8a and p62 was detected in *Vps11* or *lt* mutants and in *Vps39* RNAi cells (Figure S3). Western blots confirmed the accumulation of lipidated Atg8a-II and p62 in starved *Vps11* and *lt* mutant L3 stage larvae, similar to *Vps16A* null mutants (Figure 3I). Punctate Atg8a and p62 structures also accumulated in cells lacking HOPS in well-fed larvae (Figure S4), and RNAi depletion of genes encoding HOPS subunits prevented the formation of mCherry-Atg8a– or LTR-positive, large autolysosomes in fat body cells of wandering larvae (Figure S5). These data suggested that the loss of any one of the subunits of this complex results in accumulation of autophagosomes due to impaired maturation into autolysosomes under basal, starvation-induced, or developmental autophagy. In line with these data, ultrastructural analyses detected large numbers of autophagosomes in fat bodies of starved *Vps16A*, *Vps11*, and *lt* mutants, unlike in control larvae (Figure 4, A, C, E, and G). Interestingly, small dense vesicles were also observed in all three mutants, the contents of which sometimes
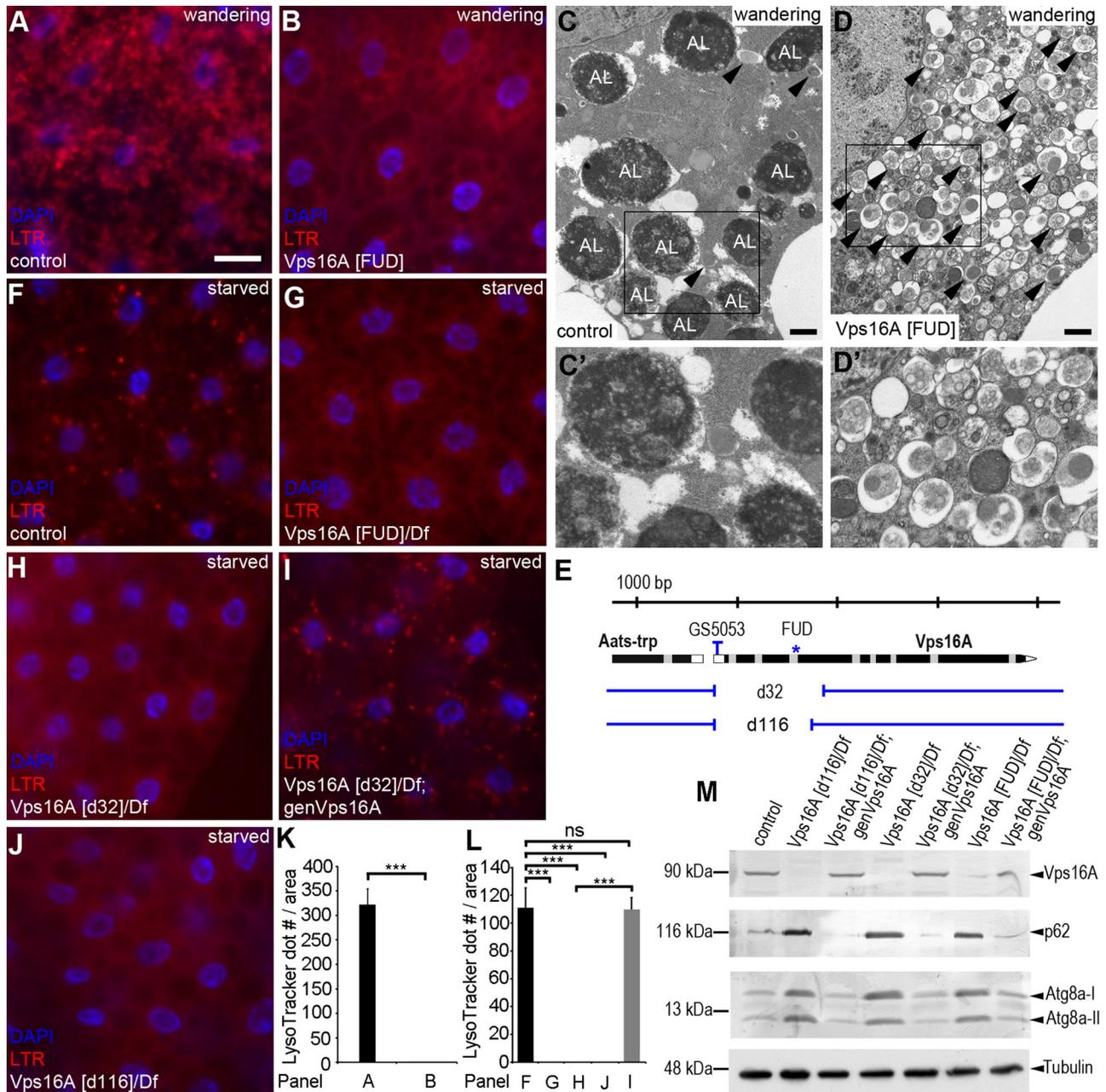
FIGURE 1: Autophagosomes accumulate in *Vps16A* mutants. (A) Large numbers of LTR-positive dots are seen in fat body cells of wandering larvae. (B) No discernible LTR dots are seen in homozygous *l(3)S007902* (*FUD*) mutant fat bodies of the same developmental stage. (C) Large-scale generation of autolysosomes (AL) is observed in fat body cells of wandering larvae. (D) Autolysosome formation is inhibited and autophagosomes (arrowheads) accumulate in large numbers in *FUD* mutant fat body cells of wandering larvae. Boxed areas in (C) and (D) are shown enlarged in (C′) and (D′). (E) Genomic map of the *Vps16A* locus. *FUD* mutants carry a point mutation at the 3′ end of the third intron (blue asterisk). The null alleles *d32* and *d116* were generated from the P element insertion *GS5053* (located in the 5′ untranslated region of *Vps16A*), and carry 1105– and 926–base pair deletions extending into the coding sequence starting from the original P element insertion site, respectively. (F–J) Three-hour starvation in a 20% sucrose solution induces punctate LTR staining in control larvae (F), unlike in hemizygous *Vps16A[FUD]* (G), *Vps16A[d32]* (H), or *Vps16A[d116]* (J) mutants. Transgenic expression of *Vps16A* restores starvation-induced LTR dot formation in *Vps16A[d32]* mutants (I). (K) Quantification of data shown in (A) and (B); *n* = 10/genotype. (L) Quantification of data shown in (F)–(J); *n* = 10/genotype. (M) Western blots reveal that Vps16A protein cannot be detected in lysates of starved *Vps16A[d32]* and *Vps16A[d116]* mutant larvae, and its level is strongly reduced in *Vps16A[FUD]* mutants. The autophagic cargo p62 and autophagosome-associated Atg8a-II accumulate to similar levels in all three mutants. Transgenic expression of *Vps16A* restores wild-type protein levels for Vps16A, p62, and Atg8a in all three mutant backgrounds. Scale bar in (A) = 20 μm for (A), (B), and (F)–(J); scale bars = 1 μm in (C) and (D). Error bars denote SE in (K) and (L); ns, not significant; ***, *p* < 0.001.
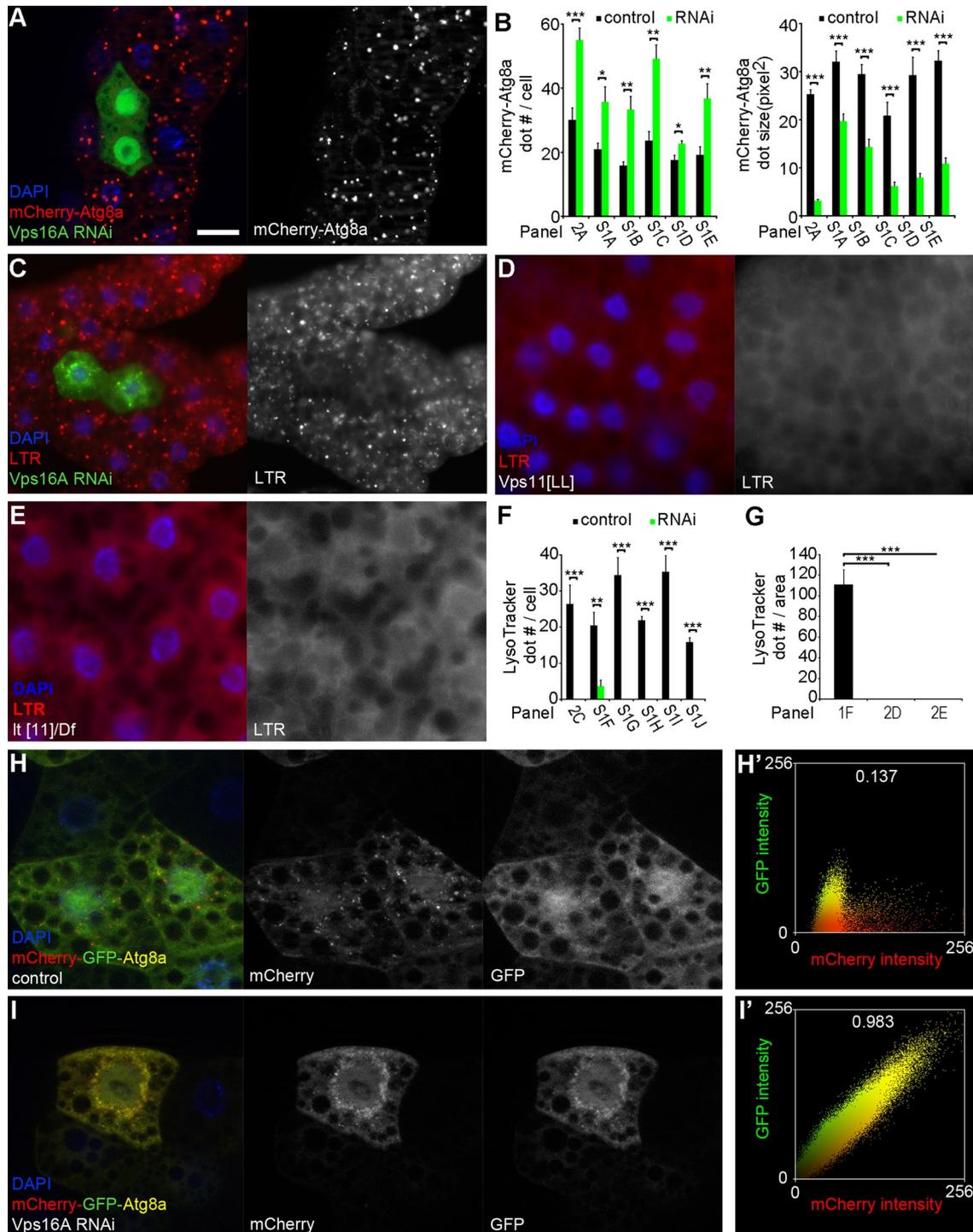
FIGURE 2: Loss of HOPS complex function leads to impaired starvation-induced autophagy. (A) Expression of a transgenic RNAi construct targeting *Vps16A* in GFP-marked clones of fat body cells causes the accumulation of small, faint, perinuclear mCherry-Atg8a dots, which are very different from the bigger, brighter puncta observed in neighboring control cells. (B) Quantification of data shown in (A) and in Figure S1, A–E; *n* = 10/genotype. (C–E) Depletion of *Vps16A* in cell clones marked by Lamp1-GFP prevents punctate LTR staining (C), compared with neighboring controls cells. Similarly, no discernible LTR structures are seen in starved *Vps11[LL]* (D) or *lt[11]* (E) mutant fat cells. (F) Quantification of data shown in (C) and Figure S1, F–J; *n* = 9/genotype for (F); *n* = 10/genotype for others. (G) Quantification of data shown in (D), (E), and Figure 1F; *n* = 10/genotype. (H and I) The double-tagged mCherry-GFP-Atg8a reporter is transported to autolysosomes, which are seen as mCherry-positive dots due to quenching of GFP in starved control cells (H). Silencing of *Vps16A* (I) results in a block of GFP quenching; thus dots appear yellow in merged images. (H') and (I') depict dot plots of intensity and colocalization profiles for the mCherry and GFP channels from (H) and (I). Numbers on top show Pearson correlation coefficients, indicating increased colocalization of GFP and mCherry in (I) compared with (H). Scale bar in (A) = 20 μm for (A), (C), (D), and (E); scale bar = 40 μm for (H) and (I). Error bars denote SE in (B), (F), and (G); ***, $p < 0.001$, **, $p < 0.01$, *, $p < 0.05$.
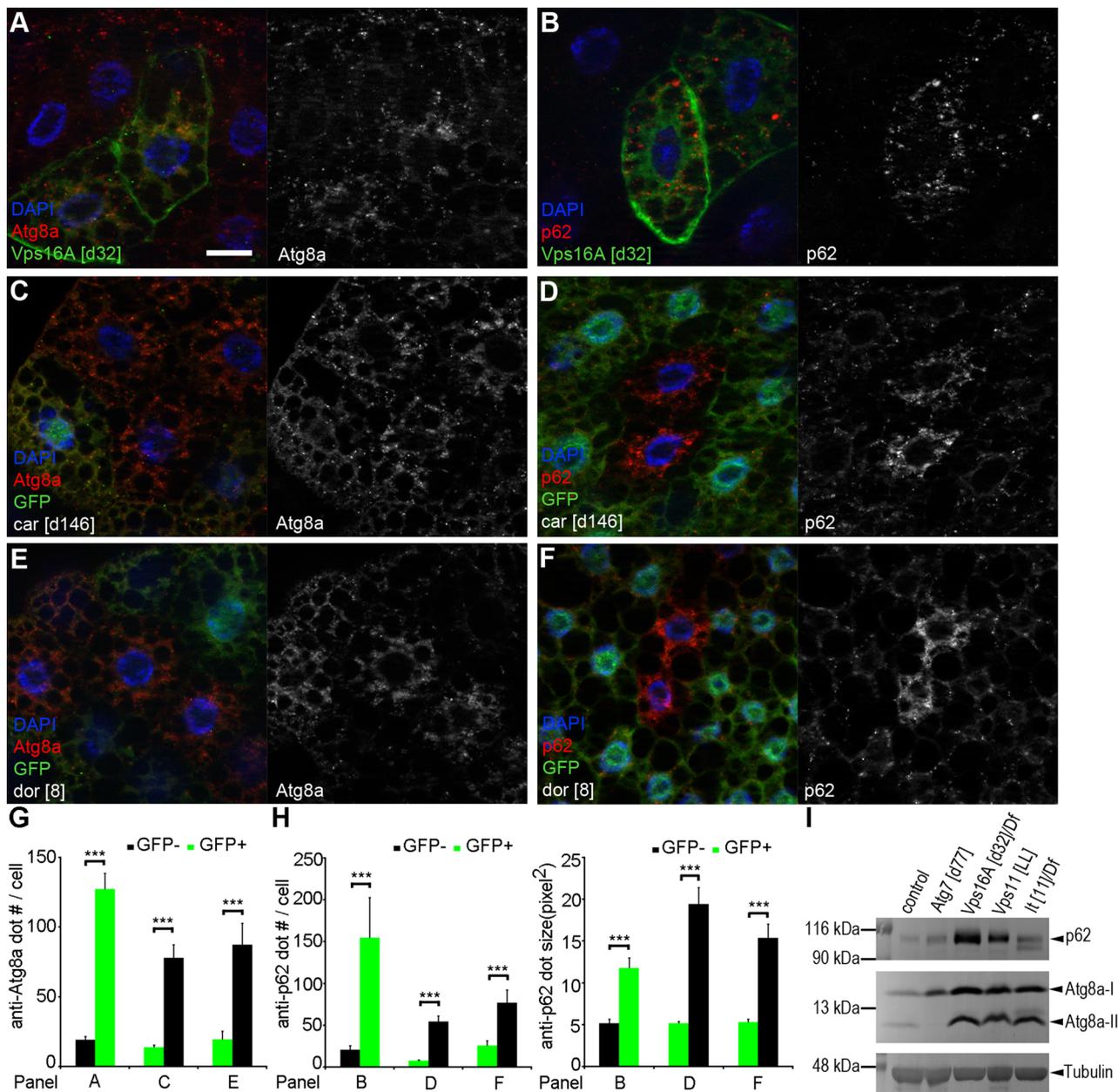
FIGURE 3: The autophagic cargo p62 and Atg8a-positive autophagosomes accumulate in starved HOPS mutants. (A–F) Endogenous Atg8a-positive autophagosomes (A, C, and E) and endogenous p62 (B, D, and F) aggregates accumulate in *Vps16A* (A and B), *car* (C and D), or *dor* (E and F) null mutant cells, compared with surrounding control fat cells in starved mosaic larvae. Note that *Vps16A* mutant cells are marked by GFP in (A) and (B), whereas *car* or *dor* mutant cells can be recognized by the lack of GFP in (C)–(F). (G) Quantification of data shown in (A), (C), and (E); n = 10/genotype. (H) Quantification of data shown in (B), (D), and (F); n = 10/genotype. (I) Western blots show that p62 and Atg8a-II are up-regulated in starved *Vps16A*, *Vps11*, and *lt* mutants compared with wild-type controls. *Atg7* mutants are used as an additional control. Scale bar in (A) = 20 μm for (A–F). Error bars denote SE in (G) and (H); ***, $p < 0.001$.

seemed to originate from sequestered cytoplasmic material (Figure 4, D, F, and H). While some of these structures likely represent aberrant autolysosomes, their size and morphology was profoundly different from autolysosomes observed in control cells, which also indicates the inefficient fusion of autophagosomes with lysosomes. Autolysosomes in control cells are much bigger and often have an irregular shape due to multiple autophagosomal fusion events, which is also evident from the heterogenity of the contents reflecting different stages of degradation within the same lytic organelle (Figure 4B).

Vps16A colocalizes with Syx17, Atg8a, and Lamp1-GFP

We and others have recently reported that Syx17, a Qa SNARE protein located on autophagosomes, is required for the fusion of these vesicles with late endosomes and lysosomes (Itakura *et al.*, 2012; Takats *et al.*, 2013). Thus we reasoned that Syx17 may cooperate with HOPS for autophagosome clearance. In line with this hypothesis, the colocalization of endogenous Vps16A with endogenous Syx17 could clearly be demonstrated in fat body cells of both control and *Vamp7* mutant larvae (Figure 5, A and B). Vps16A also localized to Atg8a-positive puncta in fat body cells of both
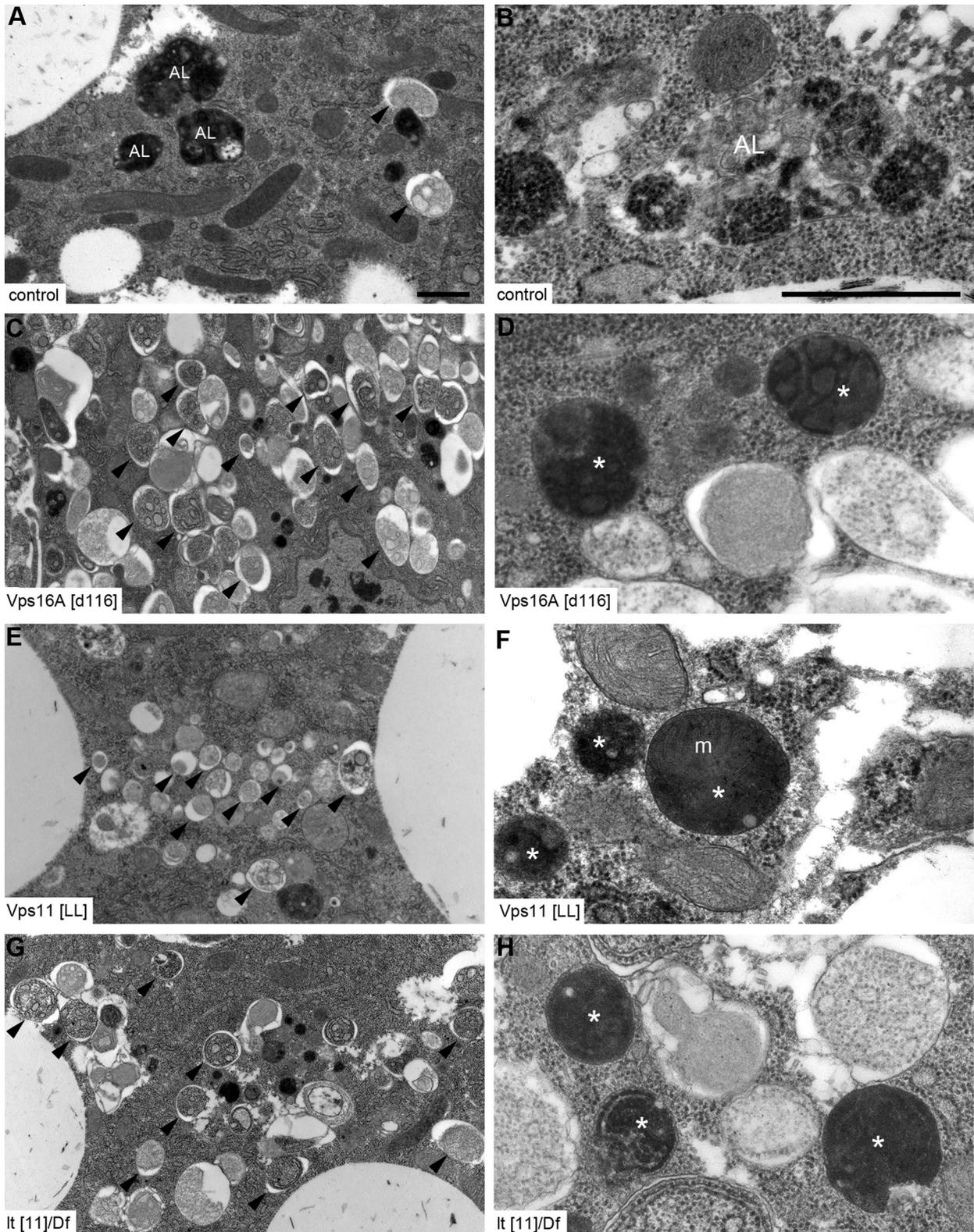
FIGURE 4: Ultrastructural analysis of starved HOPS mutants. (A) Starvation leads to the formation of autophagosomes (arrowheads) and autolysosomes (AL) in fat body cells of control larvae. (B) This panel illustrates a representative autolysosome containing heterogenous material due to different stages of degradation. Note that distinct parts within this irregularly shaped organelle can be seen, corresponding to multiple autophagosome-lysosome fusion events. (C–H) Autophagosomes accumulate in large numbers in *Vps16A* (C), *Vps11* (E), or *lt* (G) mutant cells. In addition, numerous dense organelles are seen, which are usually round and smaller than the autolysosomes observed in controls. High-magnification images reveal that a subset of these presumably lytic vesicles (marked by asterisks) in *Vps16A* (D), *Vps11* (F), or *lt* (H) mutant cells contain recognizable remnants of cytoplasmic material, such as a mitochondrion (m) in (F). Scale bar in (A) = 1 μm for (A), (C), (E), and (G); scale bar in (B) = 1 μm for (B), (D), (F), and (H).
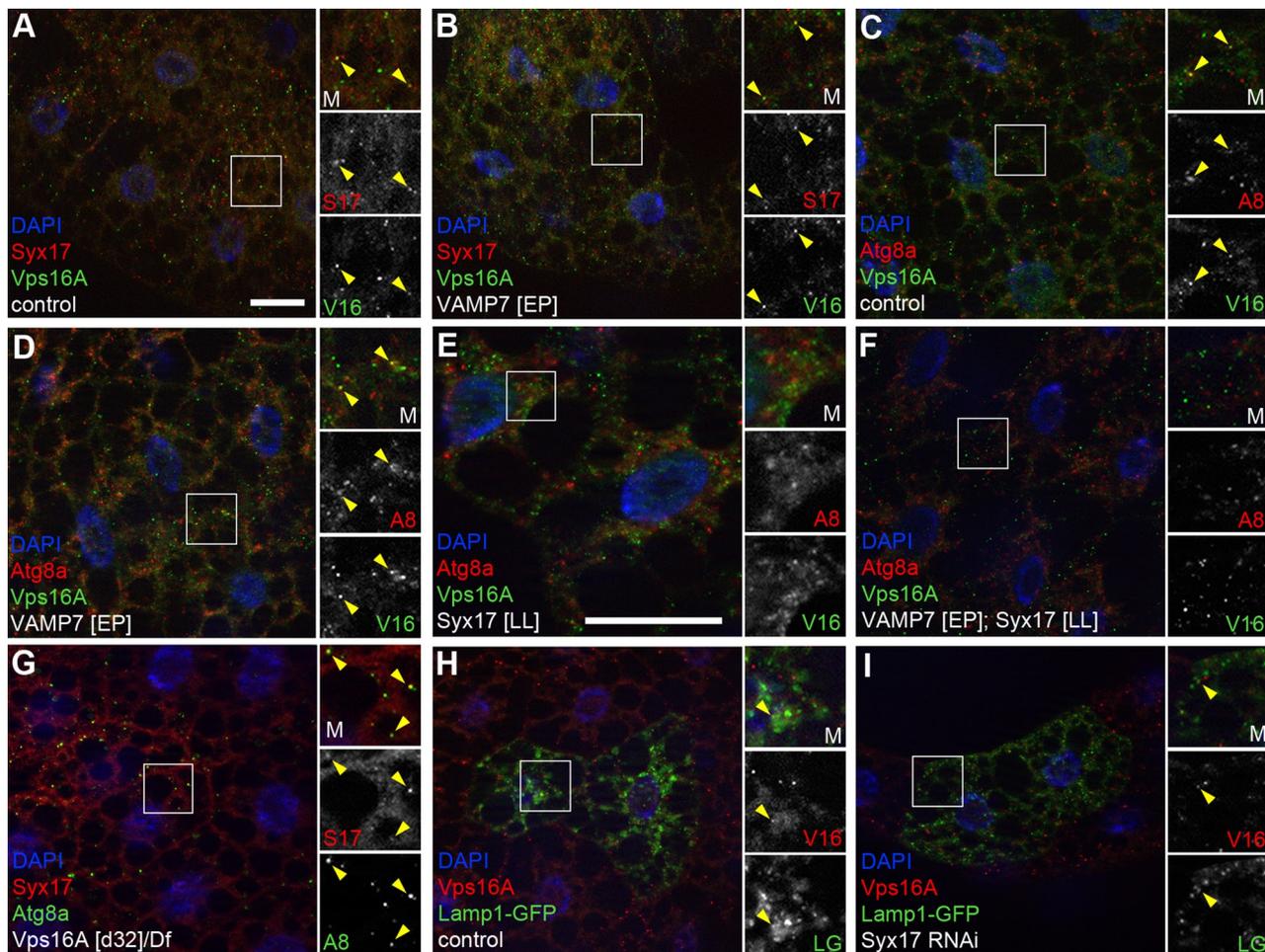
FIGURE 5: Vps16A colocalizes with the autophagosomal SNARE Syx17, the autophagosome marker Atg8a, and the lysosome reporter Lamp1-GFP in fat body cells of starved larvae. (A and B) Endogenous Syx17 colocalizes with endogenous Vps16A in starved control (A) and *Vamp7* mutant (B) fat body cells. (C–F) Vps16A localizes to endogenous Atg8a-positive structures in starved control (C) and *Vamp7* mutant (D) fat body cells. Colocalization of Vps16A with Atg8a is not seen in *Syx17* mutants (E) and *Vamp7, Syx17* double mutants (F). (G) Syx17 colocalizes with Atg8a in *Vps16A* mutants. (H and I) Vps16A colocalizes with the lysosome marker Lamp1-GFP in both starved control (H) and *Syx17* RNAi (I) fat body cells. Boxed areas are shown enlarged as indicated, with representative colocalizations highlighted by yellow arrowheads. M, merged; S17, Syx17; V16, Vps16A; A8, Atg8a; LG, Lamp1-GFP. Scale bar in (A) = 20 μm for (A)–(D) and (F)–(I); scale bar in (E) = 20 μm.

control and *Vamp7* mutant larvae (Figure 5, C and D). Vps16A colocalization with Atg8a was almost never seen in *Syx17* mutants and in *Vamp7, Syx17* double mutants (Figure 5, E and F), raising the possibility that Syx17 may have a role in the association of Vps16A with autophagosomes. Syx17 still colocalized with Atg8a in *Vps16A* mutants (Figure 5G), similar to the situation described for wild-type cells (Takats *et al.*, 2013). These data suggested that HOPS is dispensable for Syx17 loading onto autophagosomes. HOPS is also involved in homotypic vacuole/lysosome fusion in yeast, and may fulfill its function during autophagosome-lysosome fusion while associated with the surface of lysosomes. This prompted us to carry out further localization experiments. Indeed, colocalization of Vps16A with the lysosome reporter Lamp1-GFP, and with the resident lysosomal hydrolase reporter cathepsin D-mCherry could be detected in both control and *Syx17* RNAi or mutant cells (Figures 5, H and I, and S6, A and B). As expected, RNAi silencing of *Vps39* prevented the colocalization of endogenous Atg8a or Syx17 with Lamp1-GFP (Figure S6, C–F), indicating that HOPS-mediated

tethering is important for the fusion of Atg8a- and Syx17-positive autophagosomes with lysosomes.

HOPS interacts with Syx17

The similar mutant phenotypes and our colocalization experiments suggested that HOPS may bind to Syx17. Indeed, hemagglutinin (HA)-Car, Myc-Dor, and HA-Vps16A were readily coimmunoprecipitated with FLAG-Syx17 from cultured insect cells (Figure 6A). The strength of interactions seen between these overexpressed proteins was very similar, suggesting that the HOPS complex as a whole may interact with Syx17. We next tested whether the interaction of Syx17 with HOPS is enhanced by starvation, because this treatment induces autophagosome formation, and as a consequence, it also increases the number of autophagosomal fusion events. In line with this model, the interaction of endogenous Syx17 with transiently expressed Myc-Dor appeared to increase in response to starvation in adult flies (Figure 6B). A previous report showed that in yeast, the Vps33-Vam3 interaction requires Vps18 (Sato *et al.*, 2000), raising
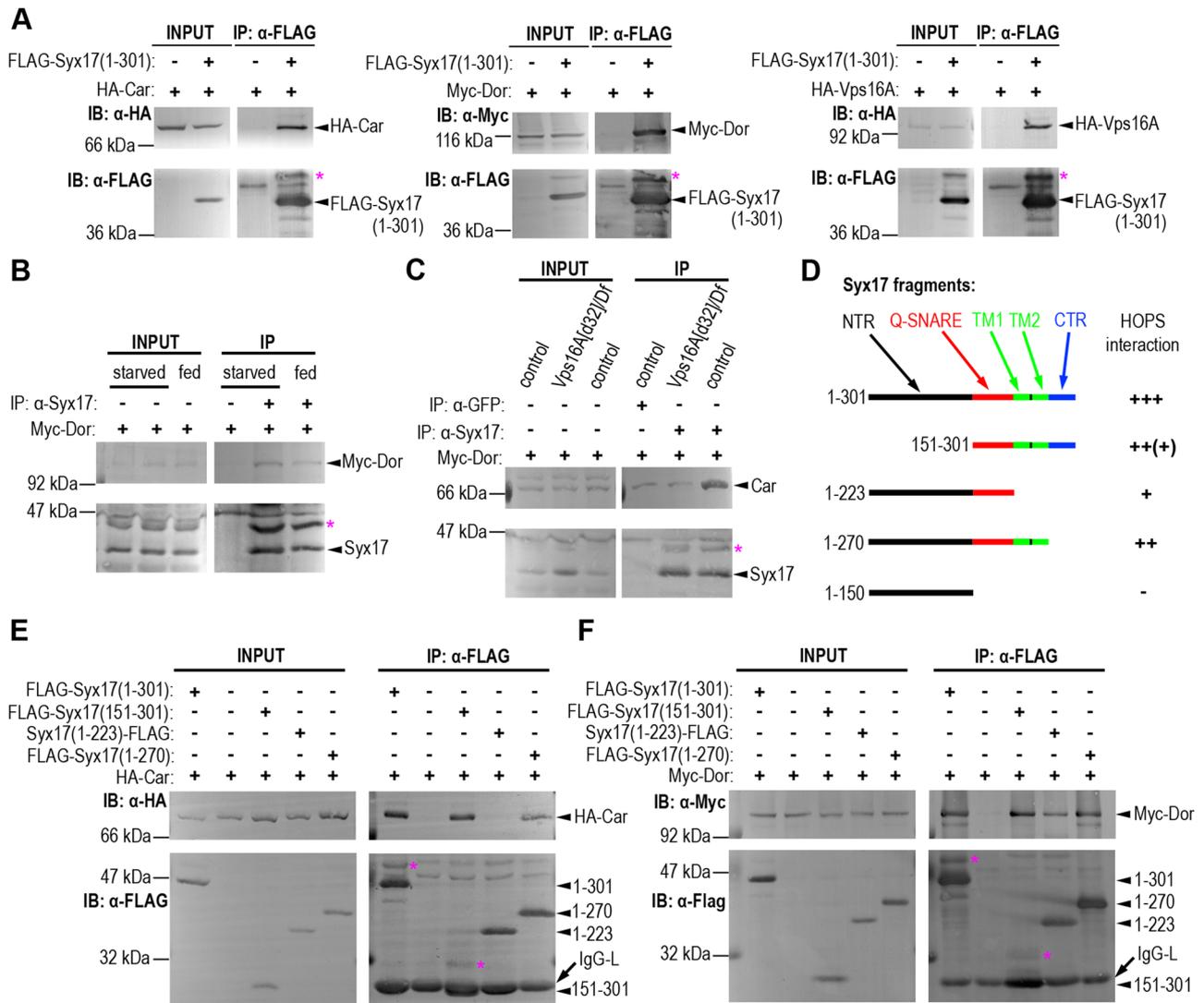
FIGURE 6: Multiple HOPS subunits interact with Syx17. (A) HA-Car, Myc-Dor, and HA-Vps16A coprecipitate with full-length FLAG-Syx17 in cultured *Drosophila* cells. (B) The interaction of transiently expressed Myc-Dor increases with endogenous Syx17 in response to starvation in immunoprecipitation experiments from adult flies. (C) Endogenous Car coprecipitates with endogenous Syx17 in starved control larvae, but not in starved *Vps16A* mutants. (D) An illustration of the truncated Syx17 fragments used in mapping experiments, together with the summary of their interactions with HOPS subunits based on experiments shown in (E), (F), and Figure S6, I and J. Abbreviations are as follows: NTR, N-terminal region; Q-SNARE, Q-SNARE domain; TM1 and 2, transmembrane domains 1 and 2, respectively; CTR, C-terminal region. Numbers refer to amino acid positions in full-length Syx17. (E and F) Immunoprecipitation analysis of HA-Car (E) and Myc-Dor (F) with FLAG-tagged Syx17 constructs shown in (D). Asterisks mark a higher-molecular-weight isoform of endogenous Syx17 in (B) and (C), which likely represents a C-terminally extended 346–amino acid protein isoform as a result of stop codon readthrough (Dunn *et al.*, 2013). Note that a higher-molecular-weight isoform (also marked by asterisks in A, E, and F) is seen in the case of tagged constructs expressing full-length and N-terminally truncated Syx17, both of which contain the full 3′ untranslated region of this gene, but not in the case of C-terminally truncated versions. IP, immunoprecipitate; IgG-L, immunoglobulin light chain.

the possibility that the HOPS complex as a whole may interact with its partner SNAREs. As Vps16 is the only subunit of HOPS that binds to Vps33 in yeast (Lobingier and Merz, 2012; Solinger and Spang, 2013), we tested whether the binding of Car/Vps33A to Syx17 depends on Vps16A in *Drosophila*. Endogenous Car coprecipitated with endogenous Syx17 in starved larvae, but this specific interaction was abolished in *Vps16A* mutants (Figure 6C), supporting the hypothesis that multiple interactions between the assembled HOPS complex and Syx17 may be required for efficient binding. RNAi depletion of *car* in cultured cells appeared to destabilize the

Syx17-Vamp7 complex (Figure S6G). Furthermore, the interaction of endogenous Syx17 with endogenous usnp (ubisnap) was decreased in hypomorphic *dor* mutant adult flies (Figure S6H), suggesting that HOPS promotes proper assembly of the Syx17/usnp/Vamp7 *trans*-SNARE complex.

In yeast, biochemical studies suggested that the Vps11, Vps16, and Vps18 subunits of HOPS in combination bind to the N-terminal region of Vam3, a Qa SNARE, whereas Vps33 was found to interact with the SNARE domains of Vam3 (Qa), Vam7 (Qc), and Nyv1 (R), but not with Vti1 (Qb) of the quaternary SNARE complex involved in

homotypic vacuole fusion (Lobingier and Merz, 2012). Given that metazoan cells rely on different SNAREs during autophagosome fusion and that sequence similarity between the Qa SNAREs Vam3 and Syx17 is limited to the SNARE domains, we attempted to map the region of Syx17 involved in binding to HOPS, using various truncated fragments expressed in cultured cells (Figure 6D). In these coimmunoprecipitation experiments, full-length FLAG-Syx17 bound slightly more effectively to HA-Car than an N-terminally truncated protein (containing the Q SNARE domains, both transmembrane regions and the C-terminus; Figure 6, D and E). This is in line with the fact that Car belongs to the Sec1/Munc18-like protein family, whose members may bind to the N-terminal region of syntaxins as well (Akbar *et al.*, 2009). Full-length and N-terminally truncated Syx17 appeared to bind equally well to Myc-Dor and HA-Vps16A, respectively (Figures 6, D and F, and S6I). Removing the C-terminal region of Syx17 seemed to slightly reduce its interaction with these HOPS subunits, whereas a C-terminally truncated fragment lacking both transmembrane domains showed strongly reduced binding to HA-Car, Myc-Dor, and HA-Vps16A (Figures 6, D–F, and S6I). Finally, we could not detect an obvious interaction between the N-terminal region of Syx17 and HA-Car, Myc-Dor, or HA-Vps16A (Figures 6D and S6J). These results raise the possibility that both the SNARE domain and membrane association of Syx17 may be required for effective interaction with HOPS.

We have recently shown that loss of Syx17 impairs starvation-induced LysoTracker staining in larval fat body cells, results in the accumulation of p62 and lipidated Atg8a, and leads to climbing defects indicating neuromuscular dysfunction in adult flies (Takats *et al.*, 2013). In line with the above mapping data, transgenic expression of Syx17 lacking its extreme C-terminal region rescued these phenotypes of *Syx17* mutants similar to full-length transgenes, unlike a Syx17 transgene missing the second transmembrane domain, which is required for its membrane association (Figure 7, A–J; Itakura *et al.*, 2012).

HOPS, but not Syx17, is required for endocytic degradation
Mutations of the HOPS complex subunits *car* or *dor* have been shown to interfere with the degradation of multiple endocytic cargo molecules in vivo, including the transmembrane proteins Bride of sevenless (Boss) and Notch in developing eyes (Sevrioukov *et al.*, 1999; Akbar *et al.*, 2009). Boss is produced by the R8 photoreceptor neuron and binds to Sevenless, a receptor tyrosine kinase located on the surface of a neighboring cell, to induce its differentiation into an R7 neuron. In control larvae, anti-Boss immunostaining shows pairs of large and small dots corresponding to the R8 apical surface and endosomes in R7 cells, respectively (Figure 8A; see also the schematic in Figure 8G). *Vps16A* and *lt* mutants accumulated large amounts of Boss, just like *car* and *dor* mutant eye disks (Figure 8, B–E). In contrast, Boss staining in *Syx17* mutant eye disks was similar to controls (Figure 8F). Our immunolabeling experiments also revealed large-scale accumulation of Notch in developing eyes lacking *Vps16A*, *lt*, *car*, or *dor*, while *Syx17* mutants were again similar to controls (Figure 8, H–M). These results suggest that Syx17 is dispensable for endocytic down-regulation of Boss and Notch in vivo.

HOPS, but not Syx17, is involved in biosynthetic transport to lysosomes
Car, *dor*, and *lt* were named after the eye color phenotypes caused by hypomorphic mutations in these genes (Lloyd *et al.*, 1998). In these mutants, the formation of lysosome-related eye pigment granules is defective compared with wild-type flies that have bright red eyes. We found that eyes composed of entirely null mutant cells

for *Vps16A* had a light orange color similar to *dor* null mutant eyes (Figure 9, A–C), while the eye color of viable *Syx17* null mutants were indistinguishable from wild-type eyes (Figure 9D). These data prompted us to further analyze the biogenesis of lysosomes in the absence of HOPS or Syx17. Lamp family proteins are heavily glycosylated and protect the lysosomal membrane from digestion by resident acidic hydrolases. As a result, Lamp proteins are continuously turned over in lysosomes (Pulipparacharuvil *et al.*, 2005). With a GFP insertion in the endogenous locus, accumulation of dLamp in Western blots of *Vps16A* mutants was evident compared with control or *Syx17* mutant larvae (Figure 9E). Cathepsin L is a resident lysosomal protease synthesized as an inactive proenzyme, and it is activated by limited proteolysis in lysosomes, during which an N-terminal portion is cleaved and degraded. Endogenous pro–cathepsin L immunoreactivity was normally very low, and practically only the mature form could be seen in Western blots of control larvae, similar to *Atg7*, *Syx17*, or *Vamp7* mutants (Figure 9F). In contrast, mutation of *Vps16A* or *Vps11* resulted in large-scale accumulation of the proenzyme (Figure 9F). Taken together, these results suggest that the HOPS complex, but not Syx17, is required for proper trafficking to and biogenesis of lysosomes.

We have also tested the role of *fob/Vps16B* (encoding a subunit of an alternative HOPS complex) in biosynthetic and autophagic transport to lysosomes, using a recently published knockout line (Akbar *et al.*, 2011). Western blots did not reveal any defects in the maturation of cathepsin L in these mutants (Figure S7A). Moreover, the levels of p62 and Atg8a-II were also similar to those of controls in lysates prepared from starved *fob* mutant larvae, suggesting proper autophagic degradation (Figure S7A).

Loss of UVRAG perturbs biosynthetic transport to lysosomes, but not autophagosome formation and fusion
It has been suggested that UVRAG, the mammalian homologue of Vps38, binds to the HOPS complex to promote both autophagy and heterophagy (Liang *et al.*, 2008). Thus we decided to extend our analysis to its *Drosophila* homologue. *UVRAG* mutants have recently been described in flies: *UVRAG[GS]*, carrying a transposon insertion in the 5′ untranslated region of the gene; and two deletion alleles, *UVRAG[B7]*, removing the first exon and a small part of the second one; and *UVRAG[B21]*, removing the first exon and most of the second one (Lee *et al.*, 2011). In addition, we identified another transposon-bearing line, *UVRAG[LL]*, which is inserted at nucleotide 66 of the protein-coding sequence downstream of the translation start site ATG. In our initial genetic characterization, *UVRAG[B21]* and *UVRAG[LL]* mutants died as L3-stage larvae in *trans* with a large deficiency for this region or when crossed to each other, suggesting these alleles represent genetic nulls (Figure S7B). Hemizygous *UVRAG[B7]* larvae also died in the L3 stage, while some of the homozygotes survived until puparium formation, and *UVRAG[GS]* mutants died as pupae, indicating these alleles are strong hypomorphs (Figure S7B). *UVRAG* was recently reported to be required for endocytic degradation of multiple receptors in developing eyes (Lee *et al.*, 2011), which we also confirmed for Notch (Figure S7C). We then generated null mutant fat-cell clones for *UVRAG[B21]* and *UVRAG[LL]* and carried out standard tests for autophagy. No statistically significant alterations were detected in starvation-induced LTR or anti-Atg8a staining in these mutant cells compared with surrounding wild-type tissue (Figures 10, A–D, and S7, D and E). In the case of p62, the number of aggregates was similar in mutant and control cells, while their size was increased in mutant cells (Figures 10, E and F, and S7F). In line with these, Western blots showed that the level of lipidated Atg8a was slightly elevated in *UVRAG* mutants
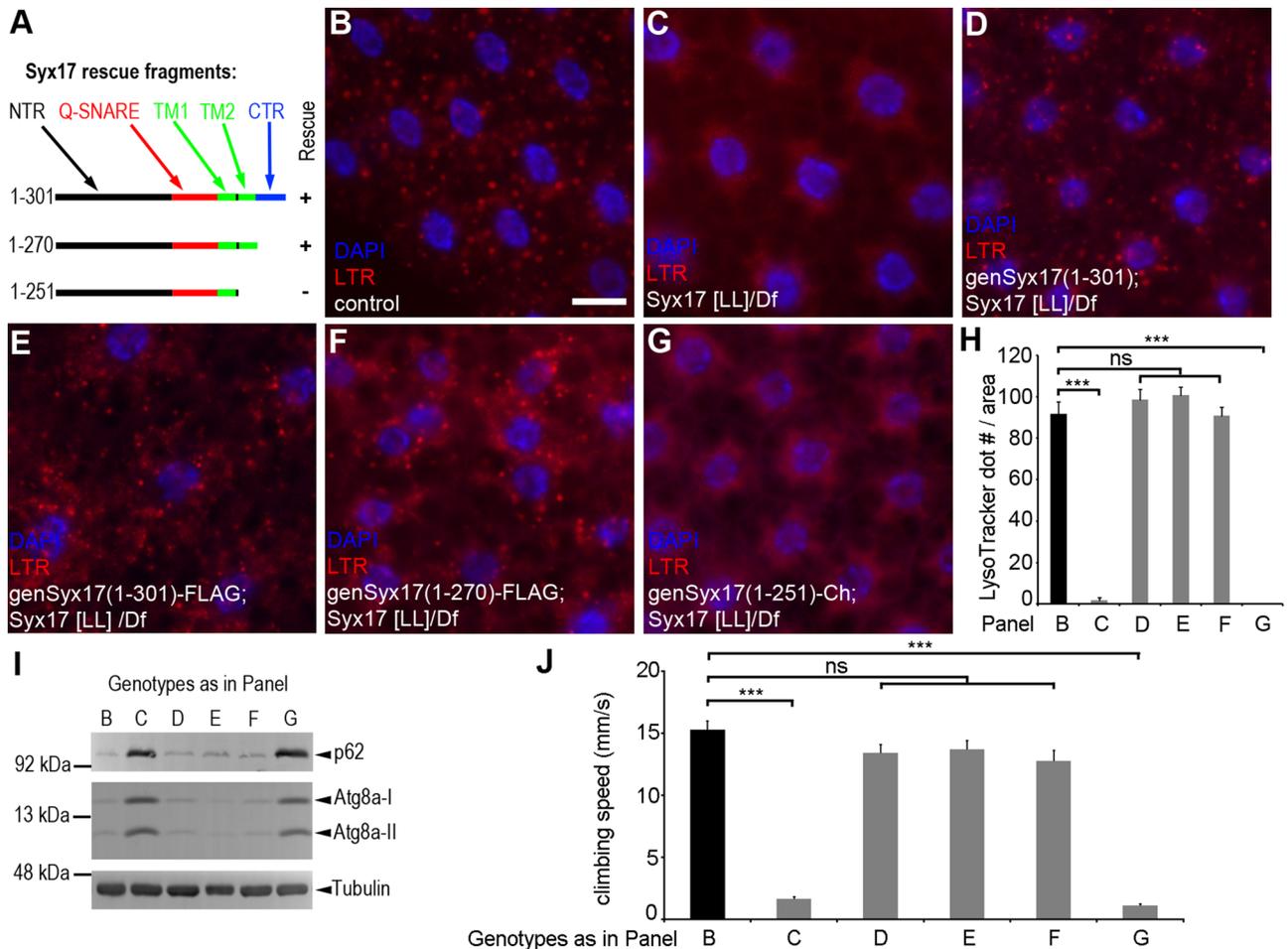
FIGURE 7: Genetic rescue experiments using truncated Syx17 fragments. (A) An illustration of the various Syx17 transgenes used in genetic rescue experiments. Please see Figure 6D for abbreviations. (B–G) LTR staining of fat body cells dissected from starved larvae. Punctate LTR staining seen in control cells (B) is missing from *Syx17* mutants (C). Both untagged (D) and C-terminally FLAG-tagged (E) full-length transgenes restore LTR dot formation in *Syx17* mutants, similar to a Syx17 fragment lacking the C-terminal region (F). A Syx17 construct lacking the second transmembrane region and C-terminus is unable to restore punctate LTR in *Syx17* mutants (G). Please note that the C-terminus of this last construct is tagged with mCherry, but the expression of this transgene is under direct control of the *Syx17* promoter, similar to the other constructs. This results in a very low expression level; therefore its fluorescence does not interfere with LTR staining. (H) Quantification of data shown in (B)–(G); $n = 10$/genotype. (I) Western blots of well-fed adult flies also show that a Syx17 fragment lacking the C-terminal region fully rescues the p62 and Atg8a-II accumulation phenotypes of well-fed *Syx17* mutant adult flies, similar to full-length transgenes. Truncating Syx17 after the first transmembrane domain prevents the rescue of these defects. (J) Negative geotaxis assays of adult flies reveal that both full-length transgenes and a Syx17 fragment lacking the C-terminal region fully rescue the climbing defects of *Syx17* mutant adult flies. Again, truncating the second transmembrane domain and C-terminus of Syx17 prevents rescue; $n = 90$ for all genotypes. Scale bar in (B) = 20 μm for (B)–(G). Error bars denote SE in (H) and (J); ns, not significant; ***, $p < 0.001$.

compared with controls, and p62 was up-regulated (Figure 10G). Ultrastructural analyses showed no accumulation of autophagosomes in *UVRAG[LL]* or *UVRAG[B21]* mutants (Figure 10, H and I). Autolysosomes were formed in these cells and had an irregular shape similar to those observed in control cells, indicating that multiple autophagosome-lysosome fusions have occurred. Interestingly, autolysosomal contents showed homogenous density, and more advanced stages of degradation were never seen in *UVRAG* mutants after 3 h of starvation, unlike in control cells. On the basis of these morphological analyses, we hypothesized that lysosomal function may be perturbed by loss of UVRAG. Indeed, pro-cathepsin L could be readily detected in Western blots of larval lysates,

although its level was much lower than that observed in *Vps16A* null mutants (Figure 10G). Moreover, the lysosome reporter Lamp1-GFP accumulated in *UVRAG* mutant cells (Figures 10J and S7G). Finally, eyes composed entirely of *UVRAG* mutant tissue showed a color different from wild-type flies, although again it was not as severe as seen in cases of *Vps16A* or *dor* mutant eyes (Figure 10, K and L). The eye color defect of *UVRAG[LL]* mutants was even more obvious in the presence of a *white[+mC]* transgene in a *white* null mutant background, which creates a hypomorphic condition regarding eye color. In these experiments, the eye color of control flies was orange, and *UVRAG* mutants had a lighter eye color (Figure 10M). These results support a conclusion that *UVRAG* plays a role in heterophagy and
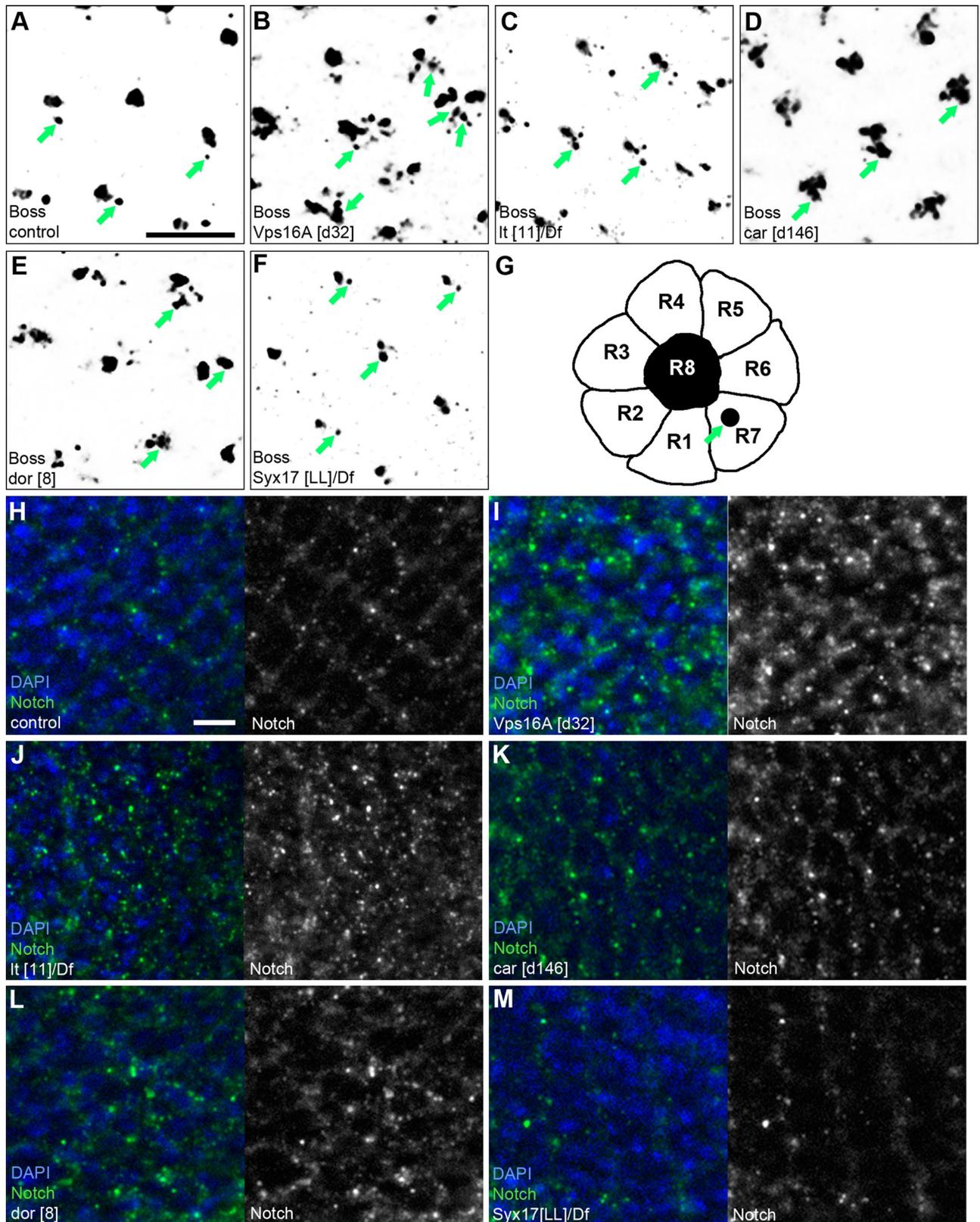
FIGURE 8: HOPS, but not Syx17, is required for endocytic down-regulation of Notch and Boss in developing eyes. (A–F) Anti-Boss staining reveals pairs of bigger and smaller dots corresponding to R8 and R7 photoreceptor neurons in the differentiating retina in control larvae (A), as indicated in the schematic (G). Accumulation of Boss is obvious in *Vps16A* (B) and *lt* (C) mutants, and also in developing eyes entirely composed of *car* (D) and *dor* (E) null mutant cells. Boss distribution in *Syx17* mutants (F) is similar to controls. (H–M) Punctate anti-Notch immunolabeling reveals a regular pattern of developing ommatidia in eye disks of control larvae (H). Mutation of *Vps16A* (I), *lt* (J), *car* (K), or *dor* (L) leads to large-scale accumulation of Notch. The level and localization of Notch in *Syx17* mutants (M) is similar to controls. Scale bar in (A) = 20 μm for (A)–(F); scale bar in (H) = 20 μm for (H)–(M).
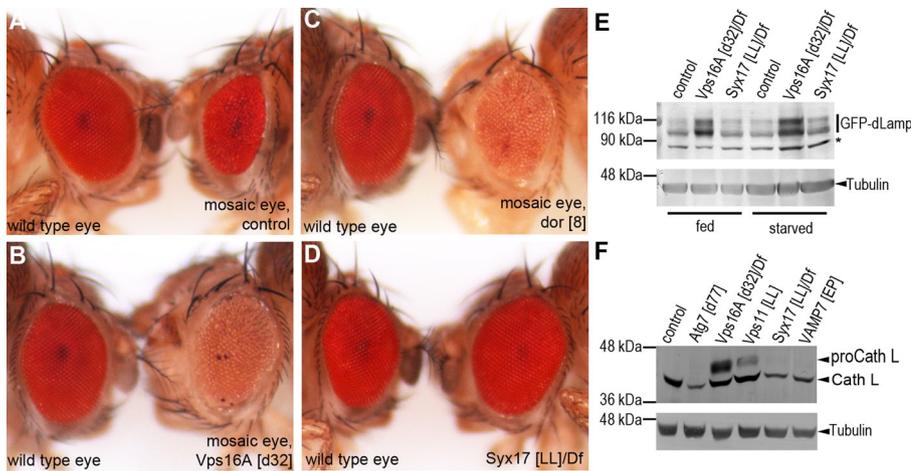
FIGURE 9: HOPS, but not Syx17, is required for biosynthetic transport to lysosomes and pigment granules. (A–D) Eye pigment granules, a type of lysosome-related organelle, are responsible for the bright red color of wild-type eyes (A). Eye tissue homozygous for one chromosome arm can be generated with the GMR-Hid method by eliminating nonhomozygous tissue due to eye-specific expression of the proapoptotic gene *Hid* in mosaic eyes. The right side (A) shows the eyes of flies entirely homozygous for a chromosome arm bearing a GFP insertion, which serves as an additional control for mosaic eye experiments. Note that the GMR-Hid method results in a rough eye phenotype, but it does not affect eye color. Eyes composed of entirely mutant cells for *Vps16A* (B) or *dor* (C) have a much lighter, orange color. The eye color of homozygous, viable *Syx17* mutants (D) is similar to that of wild-type flies. (E) Western blot using a GFP knock-in line of endogenous dLamp reveals that this lysosomal membrane protein accumulates in *Vps16A* mutant larvae, whereas no difference is seen between *Syx17* mutant and control larvae. Asterisk indicates a nonspecific band that serves as an additional loading control. (F) The proform of the resident lysosomal hydrolase cathepsin L accumulates in *Vps16A* and *Vps11* mutant larvae compared with controls, but not in *Atg7*, *Syx17*, or *Vamp7* mutants.

proper biogenesis of lysosomes. As a result, its loss likely causes a delay in autolysosomal degradation without affecting earlier steps of autophagy.

DISCUSSION

Our data presented here clearly show that all six subunits of the HOPS complex are important for the clearance of autophagosomes, acting in a cell-autonomous manner in *Drosophila*. HOPS likely promotes the fusion of autophagosomes with late endosomes and lysosomes through its interaction with Syx17, the autophagosomal SNARE. The HOPS subunit Vps16A colocalizes with Syx17 in both control and *Vamp7* mutant cells, suggesting the interaction of HOPS with Syx17 may not necessarily require formation of the Syx17-usnp-Vamp7 *trans*-SNARE complex. Supporting this hypothesis, Vps16A colocalized with Atg8a not only in control cells but also in *Vamp7* mutants, in which the fusion of autophagosomes with lysosomes is inhibited (Takáts *et al.*, 2013). The presence of Vps16A on lysosomes appears to be independent of Syx17, consistent with the known roles of HOPS during homotypic fusion of vacuoles/lysosomes. Our data are compatible with the model in which HOPS is associated with the lysosome and tethers an autophagosome moving into proximity. Interestingly, HOPS was also shown to bind various phospholipids with high affinity, including the autophagosome- and endosome-specific phosphatidylinositol 3-phosphate (Stroupe *et al.*, 2006). This is in line with our results, which suggest that the membrane association of Syx17 may increase its interaction with HOPS. Tethering is followed by formation of the *trans*-SNARE complex, which may be stabilized by HOPS during vacuole fusion in yeast as has been proposed by Starai *et al.* (2008). Finally, following fusion of

the vesicles, Syx17 is rapidly recycled from the autolysosome, as suggested by the low level of Syx17 localization to lysosomes in fly and mammalian cells (Itakura *et al.*, 2012; Takáts *et al.*, 2013).

Supporting our results and conclusions, a study related to ours shows that small interfering RNA (siRNA) silencing of *Vps33A*, *Vps16*, or *Vps39* in cultured human cells results in the accumulation of autophagosomes due to impaired fusion of these vesicles with late endosomes and lysosomes. Subunits of the HOPS complex have also been found to interact with STX17, the mammalian homologue of Syx17 in that study, suggesting a similar HOPS-dependent fusion mechanism facilitates the clearance of autophagosomes in *Drosophila* and mammals.

Unlike HOPS, which is involved in homo- and heterotypic vacuole fusion, CORVET is thought to function at the level of early endosomes in yeast, but the existence of this complex has not been verified in metazoans yet. The putative alternative HOPS complex found in animal cells, which contains Vps16B and Vps33B, has been speculated to play a role similar to that of CORVET (Balderhaar and Ungermann, 2013). Recently the *Drosophila Vps16B* homologue *fob* has been shown to be required for the maturation of bacteria-containing phagosomes but not for general endocytosis or starvation-induced LTR staining (Akbar *et al.*, 2011). Accordingly, we found no defects in lysosomal processing of cathepsin L, or in the degradation of Atg8a and p62 during autophagy in *fob* mutants. These results further confirm the distinct and specific roles of a Vps16A- and Car-containing HOPS complex in heterophagy, autophagy, and lysosome biogenesis.

The role of UVRAG in autophagy has been controversial. The yeast homologue of this gene, *VPS38*, is classified as a member of the class A *VPS* group (Bowers and Stevens, 2005). Its mutation leads to secretion of CPY without affecting vacuolar morphology, suggesting that the effect on vacuolar protein sorting may be relatively mild. Vps38/UVRAG is a subunit of a Vps34-containing lipid kinase complex both in yeast and mammals (Kihara *et al.*, 2001; Itakura *et al.*, 2008; Matsunaga *et al.*, 2009; Farre *et al.*, 2010). These studies showed that the mutually exclusive presence of Atg14 or UVRAG in distinct Vps34 complexes specifies a role in autophagosome formation or endocytosis, respectively. UVRAG has also been identified as a potential binding partner of HOPS, and based on overexpression experiments, it has been suggested as a promoter of both autophagic and endocytic degradation (Liang *et al.*, 2008). Recently *Drosophila* UVRAG was found to be required for the degradation of multiple receptors during eye development (Lee *et al.*, 2011), which we also confirmed. However, we found no defects in the formation of autophagosomes and their fusion with lysosomes in two independent cases of *UVRAG* null mutant alleles, based on multiple standard autophagy assays. The accumulation of both procathepsin L and the lysosomal membrane protein Lamp1, and defective eye pigment granule formation in *UVRAG* mutants are similar to but weaker than the phenotypes observed with HOPS mutants.

In fact, all the phenotypes of *Drosophila UVRAG* mutants may be explained by the role of this protein as a Vps34 lipid kinase subunit, which is important for endocytosis and biosynthetic transport to lysosomes (Juhasz *et al.*, 2008). Our findings are consistent with yeast studies that documented vacuolar protein–sorting defects but found no perturbation of autophagosome formation or clearance in *UVRAG* mutants (Farre *et al.*, 2010). Our data also suggest that the loss of UVRAG only influences a late step of autophagy by delaying the degradation of sequestered cargo in autolysosomes. Similarly, siRNA depletion of UVRAG blocked endocytic degradation of EGFR, but it did not affect autophagosome formation or fusion in cultured mammalian cells (Knaevelsrud *et al.*, 2010; Jiang *et al.*, 2014).

Taken together, our studies clearly establish the role of HOPS in facilitating the Syx17-dependent fusion of autophagosomes with endosomes and lysosomes in *Drosophila*, and clarify that the effect of UVRAG on autophagic degradation is likely due to perturbed biosynthetic transport of hydrolases to lysosomes.

MATERIALS AND METHODS

Drosophila genetics, treatments, and climbing tests

Flies were reared on standard yeast/cornmeal medium, and L3 stage larvae of the age 80–88 h after egg laying were transferred to a 20% sucrose solution for 3 h in starvation experiments. *Drosophila* mutants and transgenics used in this study are *l(3)S007902* bearing the *Vps16A[FUD]* allele (Szeged Stock Center, Hungary); Gal4-responsive transgenic UAS-RNAi lines for *Vps16A[GD13782], car[GD1397], dor[KK102176],* and *Vps39[GD12152], Vps11[KK102566]* (all obtained from the Vienna Drosophila RNAi Center, Vienna, Austria); *car[12230R-1]* (referred to as RNAi/2, obtained from the National Institute of Genetics, Mishima, Japan); and *lt[HMS00190]* (obtained from the Bloomington Drosophila Stock Center [BDSC], Indiana University, Bloomington, IN; and generated by the Transgenic RNAi Project, Harvard Medical School, Boston, MA). Mosaic eyes composed of entirely mutant tissue for *car, dor,Vps16A,* and *UVRAG* were generated with the help of *GMR-Hid, FRT19A; ey-Gal4, UAS-Flp* or *GMR-Hid, FRT40A; ey-Gal4, UAS-Flp* or *ey-Gal4, UAS-Flp; FRT82B, GMR-Hid* (BDSC), as previously described (Rusten *et al.*, 2007; Juhasz *et al.*, 2008). Mutant and deficiency lines used were *car[d146]* on *FRT19A* (Akbar *et al.*, 2009); *dor[4], dor[8]* on *FRT19A* (Sevrioukov *et al.*, 1999); *lt[11]* (Wakimoto and Hearn, 1990); *Df(2L)lt45, Df(3L)Exel8098, Df(3R)BSC507,* and *Df(3R)ED5339* (all obtained from BDSC); *Df(2L)ED784, UVRAG[GS17330]* (Lee *et al.*, 2011); *dLAMP[CPTI001775], Syx17[LL06330]* on *FRT2A* (Takats *et al.*, 2013); *Vps11[LL06553], UVRAG[LL03097]* on *FRT40A* (Schuldiner *et al.*, 2008) (all obtained from the Drosophila Genetic Resource Center [DGRC], Kyoto, Japan); *Atg7[d77]* (Juhasz *et al.*, 2007); *fob[1]* (Akbar *et al.*, 2011); and *UVRAG[B7], UVRAG[B21]* on *FRT40A* (Lee *et al.*, 2011) (kindly provided by Sekyu Choi). *Vps16A[d32]* and *Vps16A[d116]* were generated by imprecise excision of *Vps16A[GS5053]* (obtained from DGRC) and recombined onto *FRT82B* for generation of mutant clones. New transgenic flies were generated by standard embryo injection technique (BestGene, Chino Hills, CA). Transgenic animals for full-length, untagged genomic Syx17 have been described (Takats *et al.*, 2013). LTR and 4′,6-diamidino-2-phenylindole staining, autophagy reporter lines, and the generation of mosaic animals were described previously (Rusten *et al.*, 2004, 2007; Scott *et al.*, 2004; Juhasz *et al.*, 2007, 2008; Erdi *et al.*, 2012; Pircs *et al.*, 2012; Takats *et al.*, 2013), with the exception of positively marked (by expression of GFP) mutant clones. For these experiments, we recombined the *Vps16A[d32]* mutation onto an *FRT82B* chromosome, and also established a stock with the following genotype: *hsFlp[22]; QUAS-mCD8-GFP[5J]; ET49-QF,*

FRT82B, tub-QS[21]/TM6B, Tb (Potter *et al.*, 2010). After crossing these two lines, we generated mosaic clones by heat shocking 0- to 4-h-old embryos in a 37°C water bath, similar to generation of negatively marked (by lack of GFP or dsRed expression) mutant clones described previously (Rusten *et al.*, 2007; Juhasz *et al.*, 2008). Climbing tests were carried out on cohorts of six 2-d-old adult flies, as described previously (Juhasz *et al.*, 2007; Takats *et al.*, 2013).

Molecular cloning

The genomic rescue construct for *Vps16A* was made by cloning a 10.5-kb *Asp*718-*Bgl*II fragment containing the *Vps16A* locus into Casper4. For tagged transgenes expressed by their endogenous promoters, we generated genCherry and gen3×FLAG cloning vectors. First, a fragment containing UAS sequences, the minimal Hsp70 promoter, and multiple cloning site of UAST was removed by *Sph*I-*Xba*I digestion and replaced with a PCR-amplified *Sph*I-*Nhe*I fragment in which *Sph*I, *Not*I, *Asc*I, *Xba*I, and *Acc*65I restriction sites are upstream of an mCherry coding sequence and an *Eco*RI site is downstream of the stop codon of mCherry. Two PCR-amplified genomic fragments (*Sph*I-*Nhe*I) were cloned into *Sph*I-*Xba*I–digested genCherry vector: a 2001–base pair fragment for full-length cathepsin D containing the promoter, two exons, and the intron, and lacking the stop codon; and a 1649–base pair fragment of the genomic region of Syx17 truncated after the first transmembrane domain. The gen3×FLAG vector was generated by replacing the *Acc*65I-*Eco*RI mCherry coding fragment of genCherry with 3×FLAG, using annealed synthetic oligos. A 1799–base pair fragment of the genomic region encoding full-length Syx17 lacking the stop codon and a 1706–base pair fragment encoding Syx17 truncated after the second transmembrane domain were cloned as *Not*I-*Acc*65I fragments into gen3×FLAG digested with *Not*I-*Acc*65I. N-terminally tagged Syx17 expressing UAS constructs was generated by cloning PCR-amplified Syx17 coding sequences into UAS-3×FLAG; and N-terminally HA-tagged Vps16A-, Car-, and Vamp7-expressing constructs were generated by cloning the PCR-amplified cDNA fragments encoding full-length proteins into UAS-3×HA.

Cell culture and immunoprecipitation

Transfections and immunoprecipitations were carried out in D.mel-2 cells exactly as previously described (Takats *et al.*, 2013), using the plasmids MT-Gal4, UAS-Syx17(1-223)-FLAG (Takats *et al.*, 2013); UAS-Myc-Dor (Sevrioukov *et al.*, 1999); and N-terminally FLAG-tagged Syx17 and HA-tagged Vps16A, Car, and Vamp7 constructs described above. RNAi depletion of *car* was induced by adding 10 μg dsRNA to cultured cells in one well of a six-well plate 3 d before transfection with tagged Syx17 and Vamp7 plasmids. The dsRNA was synthesized by PCR amplification of the same region that is used in *car[12230R-1]* with specific primers containing a T7 promoter, and using the PCR fragment for in vitro transcription with the Megascript T7 kit (Life Technologies, Budapest, Hungary) followed by a clean-up reaction with the Megaclear kit (Life Technologies) and agarose gel electrophoresis to determine dsRNA integrity and quantity. Immunoprecipitations using guinea pig antisera against endogenous Syx17 (or GFP) were carried out from larval or adult fly lysates as previously described (Takats *et al.*, 2013).

Antibodies, immunolabeling, and Western blots

Indirect immunofluorescence labeling and Western blots were carried out as described (Nagy *et al.*, 2013; Takats *et al.*, 2013), using dissected fed or starved L3 larvae for fat body experiments and wandering L3 animals for eye disk experiments. The following antibodies were used: rabbit anti-Vps16A (IF [immunofluorescence]
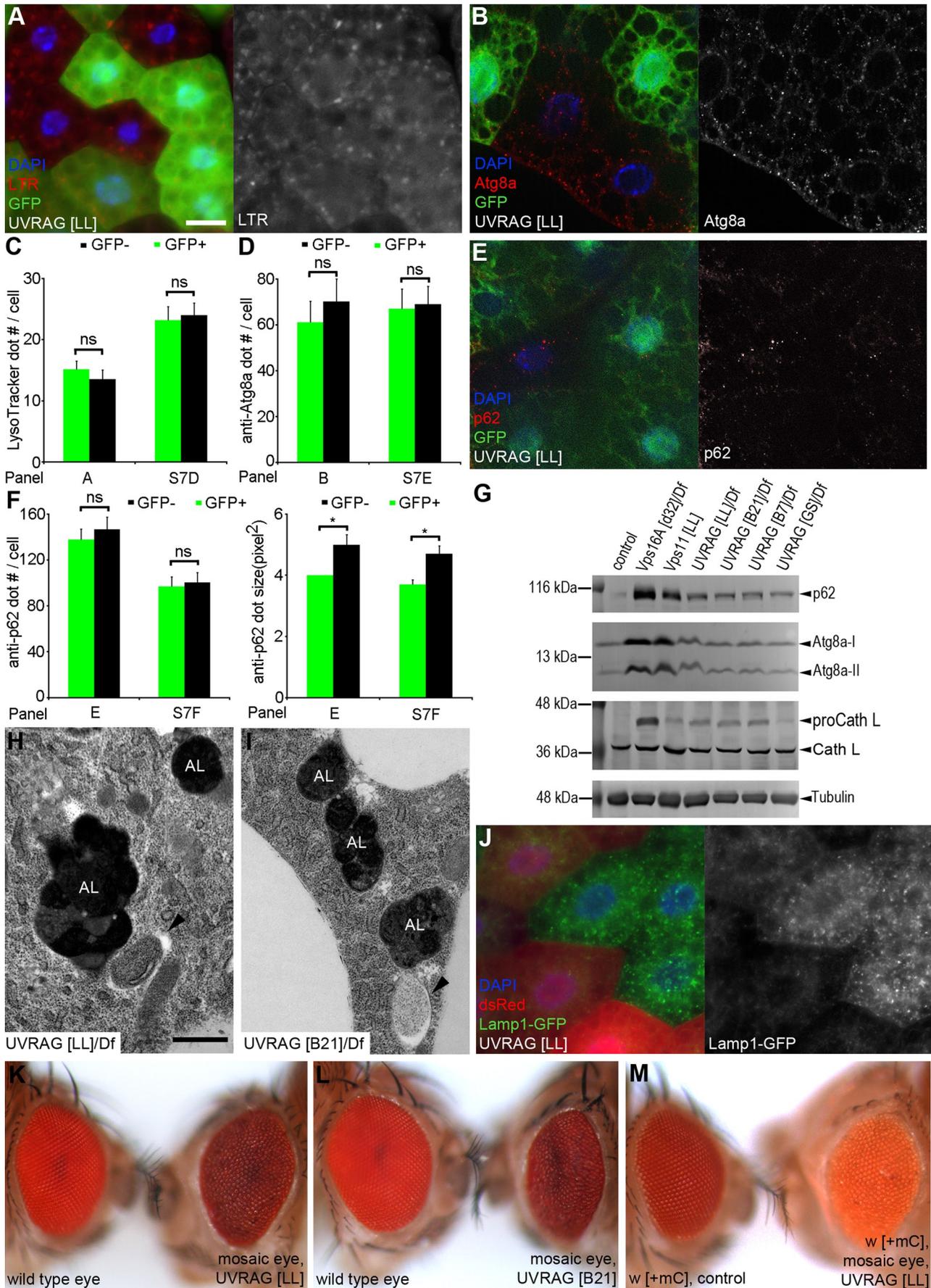
FIGURE 10: Null mutation of UVRAG has no effect on autophagosome formation and fusion, while it perturbs biosynthetic transport to lysosomes. (A) Starvation-induced punctate LTR staining in *UVRAG[LL]* mutant fat cells (marked by the lack of GFP) is similar to neighboring heterozygous (marked by expression of one copy of GFP) and homozygous (marked by two copies of GFP) control cells. (B) Atg8a-positive autophagosome numbers are similar in *UVRAG[LL]* mutant and control cells of starved larvae. (C) Quantification of data shown in (A) and Figure S7D; *n* = 10/genotype. (D) Quantification of data shown in (B) and Figure S7E; *n* = 10/genotype. (E) The autophagic cargo p62 is up-regulated in *UVRAG[LL]* mutant cells compared with surrounding control cells. (F) Quantification of data shown in (E) and Figure S7F; *n* = 10/genotype. (G) Western blots show that the levels of Atg8a-II are slightly higher in the lysates of different *UVRAG* mutant larvae than those seen in controls but are much lower than the levels seen in *Vps16A* or *Vps11* mutants. Similarly, p62 is up-regulated in *UVRAG* mutants relative to controls, but its levels do not reach those observed in *Vps16A* or *Vps11* mutants. Pro-cathepsin L accumulates in *UVRAG* mutants. (H and I) Ultrastructural analysis reveals a regular number of autophagosomes and autolysosomes in *UVRAG[LL]* (H) and *UVRAG[B21]* (I) mutant larvae in response to starvation. Note that the contents and the irregular shape of autolysosomes indicate that several autophagosomal fusion events have occurred, whereas all autolysosomes appear to contain homogenously dark material, suggesting defects in autolysosomal degradation. (J) Turnover of Lamp1-GFP (expressed in all cells) is perturbed in *UVRAG[LL]* mutant cells (marked by lack of dsRed expression), which accumulate high levels of this lysosomal reporter. (K and L) Formation of the bright red eye color observed in control flies is perturbed in animals with eyes composed of entirely *UVRAG[LL]* (K) or *UVRAG[B21]* (L) mutant tissue. (M) The dark orange eye color of flies expressing lower levels of the pigment transporter white (w) is much lighter in *UVRAG[LL]* mutant eyes. Scale bar in (A) = 20 μm for (A), (B), (E), and (J); scale bar in (H) = 1 μm for (H) and (I). Error bars denote SE in (C), (D), and (F); ns, not significant; *, $p < 0.05$.

1:300; WB [Western blot] 1:2000; Pulipparacharuvil *et al.*, 2005), rabbit anti-p62 (IF 1:2000; WB 1:5000; Pircs *et al.*, 2012), rabbit anti-Atg8a (IF: 1:500; Barth *et al.*, 2011), rabbit anti-Atg8a (WB 1:5000), rat anti-Atg8a (IF: 1:300; Takats *et al.*, 2013), mouse anti-tubulin (WB 1:1000; DSHB [Developmental Studies Hybridoma Bank, Iowa City, IA] AA4.3-s), mouse anti-FLAG M2 (WB 1:2000; Sigma-Aldrich, St. Louis, MO), mouse anti-Myc (WB 1:2000; Sigma-Aldrich), rabbit anti-HA (WB 1:2000, Sigma-Aldrich), rat anti-Syx17 (IF 1:300, WB 1:5000; Takats *et al.*, 2013), rabbit anti-Car (WB 1:1000; Akbar *et al.*, 2009), mouse anti-Notch (IF 1:50, DSHB C458.2H-c), rabbit anti-Boss (IF 1:1000; Sevrioukov *et al.*, 1999; Akbar *et al.*, 2009), rat anti-mCherry (IF 1:300), rat anti-GFP (WB 1:5000; Pircs *et al.*, 2012), chicken anti-GFP (IF 1:1500; Invitrogen, Carlsbad, CA), and rabbit anti-cathepsin L (WB 1:500; ab58991; Abcam, Cambridge, MA). Secondary antibodies were Alexa Fluor 488 goat anti-rabbit, Alexa Fluor 488 goat anti-chicken, Alexa Fluor 568 goat anti-rat, Alexa Fluor 647 goat anti-rabbit (all IF 1:1500; Invitrogen), and alkaline phosphatase–conjugated goat anti-rabbit, anti-rat and anti-mouse (both WB 1:5000; Millipore/Biocenter, Szeged, Hungary). Blots were developed using the NBT/BCIP colorimetric substrate (Sigma-Aldrich).

Microscopy and statistics

Images of dissected fat bodies were taken on an Axio Imager M2 equipped with Apotome2 and AxioCam Mrm (Zeiss, Jena, Germany), as before (Nagy *et al.*, 2013; Takats *et al.*, 2013). Autophagic structures were quantified from original, unmodified images in ImageJ (National Institutes of Health), and statistical significance was calculated with an appropriate test in SPSS Statistics (IBM, Armonk, NY), as described in detail previously (Nagy *et al.*, 2013; Takats *et al.*, 2013). Eyes of 2-d-old adults were photographed on a Lumar V12 stereomicroscope equipped with AxioCam ICc camera (Zeiss). Samples were processed for ultrastructural analysis as previously described (Erdi *et al.*, 2012; Takats *et al.*, 2013). Ultrathin sections from three individual larvae were evaluated per genotype.

REFERENCES

Akbar MA, Ray S, Kramer H (2009). The SM protein Car/Vps33A regulates SNARE-mediated trafficking to lysosomes and lysosome-related organelles. Mol Biol Cell 20, 1705–1714.

Akbar MA, Tracy C, Kahr WH, Kramer H (2011). The *full-of-bacteria* gene is required for phagosome maturation during immune defense in *Drosophila*. J Cell Biol 192, 383–390.

Balderhaar HJ, Ungermann C (2013). CORVET and HOPS tethering complexes—coordinators of endosome and lysosome fusion. J Cell Sci 126, 1307–1316.

Bankaitis VA, Johnson LM, Emr SD (1986). Isolation of yeast mutants defective in protein targeting to the vacuole. Proc Natl Acad Sci USA 83, 9075–9079.

Barth JM, Szabad J, Hafen E, Kohler K (2011). Autophagy in *Drosophila* ovaries is induced by starvation and is required for oogenesis. Cell Death Differ 18, 915–924.

Bartlett BJ *et al.* (2011). p62, Ref(2)P and ubiquitinated proteins are conserved markers of neuronal aging, aggregate formation and progressive autophagic defects. Autophagy 7, 572–583.

Bowers K, Stevens TH (2005). Protein transport from the late Golgi to the vacuole in the yeast *Saccharomyces cerevisiae*. Biochim Biophys Acta 1744, 438–454.

Csikos G, Lippai M, Lukacsovich T, Juhasz G, Henn L, Erdelyi M, Maroy P, Sass M (2009). A novel role for the Drosophila epsin (lqf): involvement in autophagy. Autophagy 5, 636–648.

Darsow T, Rieder SE, Emr SD (1997). A multispecificity syntaxin homologue, Vam3p, essential for autophagic and biosynthetic protein transport to the vacuole. J Cell Biol 138, 517–529.

Dunn JG, Foo CK, Belletier NG, Gavis ER, Weissman JS (2013). Ribosome profiling reveals pervasive and regulated stop codon readthrough in *Drosophila melanogaster*. Elife 2, e01179.

Erdi B, Nagy P, Zvara A, Varga A, Pircs K, Menesi D, Puskas LG, Juhasz G (2012). Loss of the starvation-induced gene Rack1 leads to glycogen deficiency and impaired autophagic responses in Drosophila. Autophagy 8, 1124–1135.

Farre JC, Mathewson RD, Manjithaya R, Subramani S (2010). Roles of *Pichia pastoris* Uvrag in vacuolar protein sorting and the phosphatidylinositol 3-kinase complex in phagophore elongation in autophagy pathways. Autophagy 6, 86–99.

Filimonenko M, Stuffers S, Raiborg C, Yamamoto A, Malerod L, Fisher EM, Isaacs A, Brech A, Stenmark H, Simonsen A (2007). Functional multivesicular bodies are required for autophagic clearance of protein aggregates associated with neurodegenerative disease. J Cell Biol 179, 485–500.

Ganley IG, Wong PM, Gammoh N, Jiang X (2011). Distinct autophagosomal-lysosomal fusion mechanism revealed by thapsigargin-induced autophagy arrest. Mol Cell 42, 731–743.

Hong W (2005). SNAREs and traffic. Biochim Biophys Acta 1744, 493–517.

Itakura E, Kishi C, Inoue K, Mizushima N (2008). Beclin 1 forms two distinct phosphatidylinositol 3-kinase complexes with mammalian Atg14 and UVRAG. Mol Biol Cell 19, 5360–5372.

Itakura E, Kishi-Itakura C, Mizushima N (2012). The hairpin-type tail-anchored SNARE syntaxin 17 targets to autophagosomes for fusion with endosomes/lysosomes. Cell 151, 1256–1269.

Jiang P, Nishimura T, Sakamaki Y, Itakura E, Hatta T, Natsume T, Mizushima N (2014). The HOPS complex mediates autophagosome–lysosome fusion through interaction with syntaxin 17. Mol Biol Cell 25, 1327–1331.

Juhasz G, Erdi B, Sass M, Neufeld TP (2007). Atg7-dependent autophagy promotes neuronal health, stress tolerance, and longevity but is dispensable for metamorphosis in Drosophila. Genes Dev 21, 3061–3066.

Juhasz G, Hill JH, Yan Y, Sass M, Baehrecke EH, Backer JM, Neufeld TP (2008). The class III PI(3)K Vps34 promotes autophagy and endocytosis but not TOR signaling in Drosophila. J Cell Biol 181, 655–666.

Kihara A, Noda T, Ishihara N, Ohsumi Y (2001). Two distinct Vps34 phosphatidylinositol 3-kinase complexes function in autophagy and carboxypeptidase Y sorting in Saccharomyces cerevisiae. J Cell Biol 152, 519–530.

Kimura S, Noda T, Yoshimori T (2007). Dissection of the autophagosome maturation process by a novel reporter protein, tandem fluorescent-tagged LC3. Autophagy 3, 452–460.

Knaevelsrud H, Ahlquist T, Merok MA, Nesbakken A, Stenmark H, Lothe RA, Simonsen A (2010). UVRAG mutations associated with microsatellite unstable colon cancer do not affect autophagy. Autophagy 6, 863–870.

Lee G, Liang C, Park G, Jang C, Jung JU, Chung J (2011). UVRAG is required for organ rotation by regulating Notch endocytosis in Drosophila. Dev Biol 356, 588–597.

Liang C et al. (2008). Beclin1-binding UVRAG targets the class C Vps complex to coordinate autophagosome maturation and endocytic trafficking. Nat Cell Biol 10, 776–787.

Lindmo K, Simonsen A, Brech A, Finley K, Rusten TE, Stenmark H (2006). A dual function for Deep orange in programmed autophagy in the Drosophila melanogaster fat body. Exp Cell Res 312, 2018–2027.

Lippai M, Csikos G, Maroy P, Lukacsovich T, Juhasz G, Sass M (2008). SNF4Aγ, the Drosophila AMPK γ subunit is required for regulation of developmental and stress-induced autophagy. Autophagy 4, 476–486.

Lloyd V, Ramaswami M, Kramer H (1998). Not just pretty eyes: Drosophila eye-colour mutations and lysosomal delivery. Trends Cell Biol 8, 257–259.

Lobingier BT, Merz AJ (2012). Sec1/Munc18 protein Vps33 binds to SNARE domains and the quaternary SNARE complex. Mol Biol Cell 23, 4611–4622.

Matsunaga K et al. (2009). Two Beclin 1-binding proteins, Atg14L and Rubicon, reciprocally regulate autophagy at different stages. Nat Cell Biol 11, 385–396.

Mizushima N, Levine B, Cuervo AM, Klionsky DJ (2008). Autophagy fights disease through cellular self-digestion. Nature 451, 1069–1075.

Nagy P, Varga A, Pircs K, Hegedus K, Juhasz G (2013). Myc-driven overgrowth requires unfolded protein response-mediated induction of autophagy and antioxidant responses in Drosophila melanogaster. PLoS Genetics 9, e1003664.

Peng C et al. (2012). Ablation of vacuole protein sorting 18 (Vps18) gene leads to neurodegeneration and impaired neuronal migration by disrupting multiple vesicle transport pathways to lysosomes. J Biol Chem 287, 32861–32873.

Pircs K, Nagy P, Varga A, Venkei Z, Erdi B, Hegedus K, Juhasz G (2012). Advantages and limitations of different p62-based assays for estimating autophagic activity in Drosophila. PLoS One 7, e44214.

Potter CJ, Tasic B, Russler EV, Liang L, Luo L (2010). The Q system: a repressible binary system for transgene expression, lineage tracing, and mosaic analysis. Cell 141, 536–548.

Pulipparacharuvil S, Akbar MA, Ray S, Sevrioukov EA, Haberman AS, Rohrer J, Kramer H (2005). Drosophila Vps16A is required for trafficking to lysosomes and biogenesis of pigment granules. J Cell Sci 118, 3663–3673.

Rieder SE, Emr SD (1997). A novel RING finger protein complex essential for a late step in protein transport to the yeast vacuole. Mol Biol Cell 8, 2307–2327.

Rothman JH, Stevens TH (1986). Protein sorting in yeast: mutants defective in vacuole biogenesis mislocalize vacuolar proteins into the late secretory pathway. Cell 47, 1041–1051.

Rusten TE, Lindmo K, Juhasz G, Sass M, Seglen PO, Brech A, Stenmark H (2004). Programmed autophagy in the Drosophila fat body is induced by ecdysone through regulation of the PI3K pathway. Dev Cell 7, 179–192.

Rusten TE et al. (2007). ESCRTs and Fab1 regulate distinct steps of autophagy. Curr Biol 17, 1817–1825.

Sato TK, Rehling P, Peterson MR, Emr SD (2000). Class C Vps protein complex regulates vacuolar SNARE pairing and is required for vesicle docking/fusion. Mol Cell 6, 661–671.

Schuldiner O, Berdnik D, Levy JM, Wu JS, Luginbuhl D, Gontang AC, Luo L (2008). piggyBac-based mosaic screen identifies a postmitotic function for cohesin in regulating developmental axon pruning. Dev Cell 14, 227–238.

Scott RC, Schuldiner O, Neufeld TP (2004). Role and regulation of starvation-induced autophagy in the Drosophila fat body. Dev Cell 7, 167–178.

Sevrioukov EA, He JP, Moghrabi N, Sunio A, Kramer H (1999). A role for the deep orange and carnation eye color genes in lysosomal delivery in Drosophila. Mol Cell 4, 479–486.

Solinger JA, Spang A (2013). Tethering complexes in the endocytic pathway: CORVET and HOPS. FEBS J 280, 2743–2757.

Starai VJ, Hickey CM, Wickner W (2008). HOPS proofreads the trans-SNARE complex for yeast vacuole fusion. Mol Biol Cell 19, 2500–2508.

Stenmark H (2009). Rab GTPases as coordinators of vesicle traffic. Nat Rev Mol Cell Biol 10, 513–525.

Stroupe C, Collins KM, Fratti RA, Wickner W (2006). Purification of active HOPS complex reveals its affinities for phosphoinositides and the SNARE Vam7p. EMBO J 25, 1579–1589.

Swetha MG, Sriram V, Krishnan KS, Oorschot VM, ten Brink C, Klumperman J, Mayor S (2011). Lysosomal membrane protein composition, acidic pH and sterol content are regulated via a light-dependent pathway in metazoan cells. Traffic 12, 1037–1055.

Takats S, Nagy P, Varga A, Pircs K, Karpati M, Varga K, Kovacs AL, Hegedus K, Juhasz G (2013). Autophagosomal Syntaxin17-dependent lysosomal degradation maintains neuronal function in Drosophila. J Cell Biol 201, 531–539.

Wakimoto BT, Hearn MG (1990). The effects of chromosome rearrangements on the expression of heterochromatic genes in chromosome 2L of Drosophila melanogaster. Genetics 125, 141–154.

Wang CW, Stromhaug PE, Shima J, Klionsky DJ (2002). The Ccz1-Mon1 protein complex is required for the late step of multiple vacuole delivery pathways. J Biol Chem 277, 47917–47927.